Tropolone as a pure solid exists as dimers, as can be seen in Figure 7. The explanation given above describing the motions involved in reorienting the tropolone molecule subsequent to a proton transfer invokes the simplest possible mechanism. It cannot be determined from the present NMR data whether the proton transfer occurs intramolecularly or intermolecularly. It is possible that a concerted process involving transfer of two protons (either intra or inter) would occur for a dimer, but again both of these molecules would then have to undergo an out-of-plane rotation to pack properly in the lattice. There is no other mechanism short of translation that would restore the order necessary to produce the sharp reflections observed in the X-ray experiment. In summary, it would appear likely that proton transfer in pure solid tropolone occurs very rapidly via a tunneling mechanism as is observed in matrix-isolated molecules but requires a subsequent energetically unfavorable reorientation to pack properly into the crystal lattice again. It is this latter process that determines if the product will survive and is responsible for the rate of exchange measured in the current ^{13}C NMR experiment. This is also consistent with the large energy of activation, 26 kcal/mol, measured in this set of experiments.

Acknowledgment. We are grateful to Prof. O. Anderson and C. Schauer for their help and use of the Nicolet R3m/E X-ray structure determination package for the graphics on which the packing plot was prepared. This system was purchased with funds provided by the National Science Foundation (Grant CHE 8103011). The liquid-state spectra were obtained at the Colorado State University Regional NMR Center, funded by the National Science Foundation (Grant CHE 78-18581). Partial support of this work was by the U.S. Geological Survey.

Registry No. Tropolone, 533-75-5.

Triple-Decker Sandwiches.[1] Syntheses, Reactivity, Electrochemistry, and X-ray Crystal and Electronic Structures of Bis(cyclopentadienylmetal)-μ-1,3-diborolenyl Complexes with 29–34 Valence Electrons

Joseph Edwin,[2a] Manfred Bochmann,[2a] Michael C. Böhm,[2b] David E. Brennan,[2d] William E. Geiger,*[2d] Carl Krüger,*[2c] Jürgen Pebler,[2a] Hans Pritzkow,[2b] Walter Siebert,*[2b] Wolfgang Swiridoff,[2b] Hubert Wadepohl,[2b] Johannes Weiss,[2b] and Ulrich Zenneck[2b]

Contribution from the Fachbereich Chemie der Universität Marburg, D-3550 Marburg, Federal Republic of Germany, the Anorganisch-Chemisches Institut der Universität and the Organisch-Chemisches Institut der Universität Heidelberg, D-6900 Heidelberg, Federal Republic of Germany, the Max-Planck-Institut fur Kohlenformschung, D-4330 Mülheim, Federal Republic of Germany, and the Department of Chemistry, University of Vermont, Burlington, Vermont 05405. *Received September 3, 1982*

Abstract: The methyltetraethyl and the diethyldimethyl derivatives of the Δ^4-1,3-diborolene heterocycle $C_{B2}H_6$, **6a**,**b**, were used for the synthesis of the triple-decker series $(\eta^5\text{-}C_5H_5)M(\mu\text{-}C_3B_2H_5)M'(\eta^5\text{-}C_5H_5)$, with MM′ = FeCo, CoCo, CoNi, and NiNi (30–33 valence electrons). This was achieved either by stacking the corresponding derivatives of the sandwich complexes $(\eta^5\text{-}C_5H_5)Ni(\eta^5\text{-}C_3B_2H_5)$ (**13a**,**b**) or $(\eta^5\text{-}C_5H_5)Co(\eta^5\text{-}C_3B_2H_6)$ (**18a**,**b**) with the $(C_5H_5)M$ moieties (M = Fe, Co, Ni) or by the reaction of the diborolenes with mono- and dinuclear metal complexes. The intensely colored compounds are chemically or electrolytically oxidized or reduced to the corresponding charged species. As predicted by theory the "FeCo", "$CoCo^+$", and "$NiNi^-$" species are diamagnetic and "$FeCo^+$", "CoCo", "$NiCo^+$", and "NiNi" are paramagnetic, each having one unpaired electron, whereas "NiCo" and "$NiNi^+$" have two unpaired electrons. Reduction of NiCo (**15b**) with potassium produced the quadruple-decker complex $[(\eta^5\text{-}C_5H_5)Co(\mu\text{-}C_3B_2H_5)]_2Ni$ (**20b**) in high yield. The reaction between NiCo and $Fe_2(CO)_9$ yielded several products: the carbonyl-bridged derivative $(\eta^5\text{-}C_5H_5)Co(\mu\text{-}C_3B_2H_5)Ni(CO)_3Fe(\eta^5\text{-}C_5H_5)$ (**22a**) and the triple-deckers $(\eta^5\text{-}C_5H_5)Fe(\mu\text{-}C_3B_2H_5)Co(\eta^5\text{-}C_5H_5)$ and $(\eta^5\text{-}C_5H_5)Co(\mu\text{-}C_3B_2H_5)Fe(CO)_3$. The NiNi triple-decker **14b** and $Fe_2(CO)_9$ resulted in the derivatives $(\eta^5\text{-}C_5H_5)M(\mu\text{-}C_3B_2H_5)Fe(CO)_3$ (M = Fe, Ni), $(CO)_3Fe(\mu\text{-}C_3B_2H_5)Ni(CO)_3Fe(\eta^5\text{-}C_5H_5)$ (**25b**), and the quadruple-decker $[(CO)_3Fe(\mu\text{-}C_3B_2H_5)]_2Ni$. The isomorphous structures of FeCo, NiCo, and NiNi (**17b**, **15b**, and **14b**) determined by single-crystal X-ray diffraction studies revealed the triple-decker sandwich arrangement, in which the $(C_5H_5)M$ and $(C_5H_5)M'$ moieties are η^5 bonded to the planar (±0.01 Å) μ-1,3-diborolenyl ligand. The distances Fe···Co, Ni···Co, Ni···Ni increase from 3.20 to 3.33 to 3.41 Å, respectively. The FeCo, NiCo, and NiNi complexes crystallize in the space group $P2_1/c$ with a = 8.574 (2), 8.618 (3), 8.711 (1) Å; b = 17.030 (4), 17.392 (4), 17.403 (1) Å; c = 13.408 (3), 13.334 (4), 13.385 (1) Å; β = 108.33 (1), 108.13 (3), 108.53 (1)°; V = 1858.9, 1899.3, 1923.8 Å^3, and Z = 4. The electronic structures of some of the triple-decker complexes were investigated by means of semiempirical MO calculations of the INDO type. The theoretical results are compared with some of the experimental findings. The paramagnetic complexes gave ^1H NMR spectra in the 40–150 ppm range. Mössbauer measurements on FeCo and $FeCo^+$ revealed parallels to the ferrocene/ferricenium couple. Magnetic measurements were carried out on several compounds, and the temperature dependence of the effective magnetic moment of $FeCo^+BF_4^-$ was studied. The redox properties of the neutral complexes were studied by the electrochemical techniques of dc and ac polarography, cyclic voltammetry, and controlled-potential coulometry. Each of the compounds can be oxidized or reduced in more than one reversible electron-transfer process. The broadest electron-transfer series was found with the dicobalt compound, which underwent three reversible electron-transfer reactions (2+/+/0/−) and one irreversible one (−/2−). Phase-selective ac polarography showed that the charge-transfer reactions were very rapid, suggesting no major structural reorganizations as a function of changing the overall oxidation state of the complexes.

In 1964 the existence of the triple-decker sandwich cations $(C_5H_5)_3Fe_2^+$, $(C_5H_5)_3FeNi^+$, and $(C_5H_5)_3Ni_2^+$ in the mass spectra of metallocenes was reported.[3] Despite intensive research, the only example known today with a C_5H_5 ring in a bridging position is the tricyclopentadienyldinickel cation (**1**) prepared by Werner

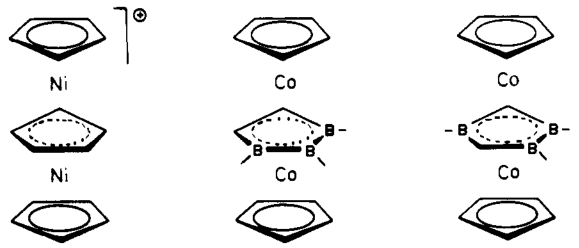

1 2 3

and Salzer[4] from nickelocene and HBF_4. Grimes et al.[5] synthesized the first neutral triple-deckers with the isomeric carboranyl rings $C_2B_3H_5$ in the μ-position. **2** and **3** each contain 30 valence electrons (VE) whereas **1** has 34 VE (electron counting in analogy to the 18 VE in ferrocene). Hoffmann et al.[6] have analyzed the electronic structure of $(C_5H_5)M(C_5H_5)M(C_5H_5)$ and $(CO)_3M(C_5H_5)M(CO)_3$ triple-deckers. Two series of stable structures with 30 and 34 VE were predicted, which led to the formulation of a 30/34 VE rule.[7] 30 VE triple-decker sandwiches with one Fe atom may be regarded as ferrocene analogues having one 12 VE stack (ligand + metal) inserted between C_5H_5 and Fe. However, the diamagnetic 34 VE triple-decker **1** does not represent the electronic extension of the paramagnetic nickelocene sandwich. Considering the MO scheme of **1**, one would expect a 32 VE species with a half-filled HOMO (e_1' for **1**) as a nickelocene analogue. The corresponding complex of cobaltocene would be a 31 VE species.

Generally, the construction of triple-decker compounds requires Lewis acid ligands in the bridging position to hold two metal complex fragments together.[8] In addition to the two-electron-donor ligands **4** and **5**, which possess no independent stability, the

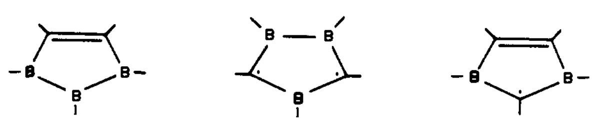

4 5 6

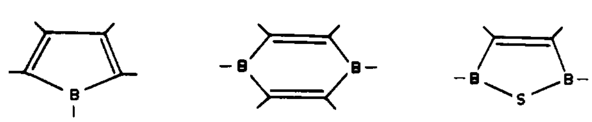

7 8 9

four-electron donors borole **7**, 1,4-diboracyclohexadiene **8**, and 1,2,5-thiadiborolene **9** have been studied. Herberich et al.[9] prepared the bis(tricarbonylmanganese) complex **10** with a borole derivative in the bridging position. The analogous complex[10] **11** was obtained with 1,2,5-thiadiborolene and $Mn_2(CO)_{10}$. **12**

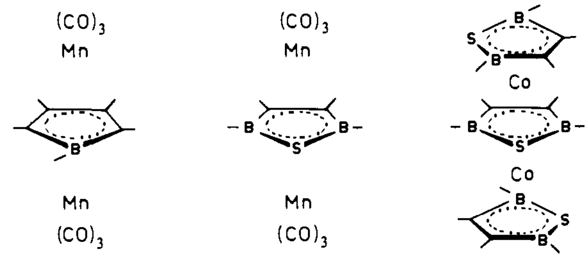

10 11 12

represents a rare type of a triple-decker sandwich, since it is entirely composed of thiadiborolene ligands.[11] Very recently[12] the first example of a complex with the six-membered ring $C_4B_2H_6$ (**8**) in the μ-position was obtained from a pentamethylcyclopentadienyl(1,4-diboracyclohexadiene)rhodium sandwich and CF_3COOH, i.e., the dication $[(C_5Me_5)Rh(C_4B_2)Rh(C_5Me_5)]^{2+}$. None of the reported triple-decker complexes[8] with the μ-ligands **4**, **5**, and **7**–**9** has more than 30 VE, in agreement with the 30/34 VE rule. We have studied not only the ligand properties of thiadiborolene **9** but also those of the 1,3-diborolene heterocycle, which after elimination of a hydrogen atom yields the three-electron ligand **6**. Since it requires three electrons to form a π^6 system, **6** reacts with $(C_5H_5)_2Ni$ or $[(C_5H_5)Ni(CO)]_2$—the source of the three-electron-donor moiety $(C_5H_5)Ni$—to the red 18 VE sandwich[13] (η^5-cyclopentadienyl)(η^5-diborolenyl)nickel **13**. Its

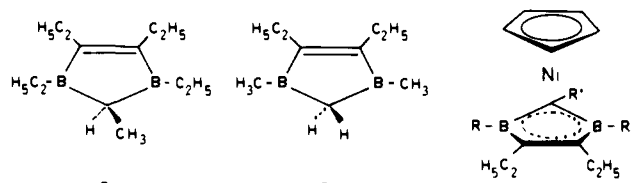

6a 6b

13a R = C_2H_5 R' = CH_3
13b R = CH_3 R' = H

strong acceptor properties toward Lewis base transition-metal complex fragments allows further reactions with $(C_5H_5)M$ moieties (M = Co Ni) to yield the first paramagnetic triple-decker complexes with 32 and 33 VE, respectively. Preliminary reports on the compounds **14a**, **15a**, and the 30 VE complex **17a** have been made.[14,15] Here we report the syntheses, structures, chemical as well as electrochemical properties, and a MO study of the complete family of 29 to 34 VE triple-decker sandwich complexes having the ligands **6a** and **6b** in the bridging position.

Results

Syntheses and Reactions. The sandwiches **13a** and **13b** react with $[(C_5H_5)Ni(CO)]_2$ in mesitylene at 140–150 °C to yield the deep green air-stable 33 VE triple-deckers **14a,b** almost quantitatively (Scheme I). They are also obtained as byproducts during the syntheses[13] of **13a,b** from the ligands **6a,b** and $[(C_5H_5)Ni(CO)]_2$ or $(C_5H_5)_2Ni$, respectively. Separation of the products is easily achieved on a silica column with *n*-hexane or petrol ether as solvent. **14a,b** sublime at 110–120 °C (0.01 torr). Similarly the paramagnetic blue-green mixed-metal triple-deckers **15a,b** with 32 VE are obtained from **13a,b** and $(C_5H_5)Co(CO)_2$ in 80–90% yield. When **15b** was sublimed from the reaction mixture of **13b** and $(C_5H_5)Co(CO)_2$, small amounts of a green complex remained

(1) Triple-Decker Complexes. 8. Part 7: Köhler, F. H.; Zenneck, U.; Edwin, J.; Siebert, W.; *J. Organomet. Chem.* **1981**, *208*, 137.
(2) (a) Universität Marburg; (b) Universität Heidelberg; (c) Max-Planck-Institut Mülheim; (d) University of Vermont.
(3) Schumacher, E.; Taubenest, R. *Helv. Chim. Acta* **1964**, *47*, 1525.
(4) Werner, H.; Salzer, A. *Inorg. Met.-Org. Chem.* **1972**, *2*, 239. Salzer, A.; Werner, H. *Ibid.* **1972**, *2*, 249. Salzer, A.; Werner, H. *Angew. Chem.* **1972**, *84*, 949.
(5) Beer, D. C.; Miller, V. R.; Sneddon, L. G.; Grimes, R. N.; Mathew, M.; Palenik, G. J. *J. Am. Chem. Soc.* **1973**, *95*, 3046.
(6) Lauher, J. W.; Elian, M.; Summerville, R. H.; Hoffmann, R. *J. Am. Chem. Soc.* **1976**, *98*, 3219.
(7) Werner, H. *Angew. Chem.* **1977**, *89*, 1.
(8) (a) Siebert, W. *Adv. Organomet Chem.* **1980**, *18*, 301. (b) Siebert, W. In "Transition Metal Chemistry"; Müller, A., Diemann, E., Eds.; Verlag Chemie: Weinheim (FRG), 1981; p 157.
(9) Herberich, G. E.; Hengesbach, J.; Kölle, U.; Huttner, G.; Frank, A. *Angew. Chem.* **1976**, *88*, 450; *Angew Chem., Int. Ed. Engl.* **1976**, *15*, 433.
(10) Siebert, W.; Kinberger, K. *Angew. Chem.* **1976**, *88*, 451; *Angew. Chem., Int. Ed. Engl.* **1976**, *15*, 434.
(11) Siebert, W.; Rothermel, W. *Angew. Chem.* **1977**, *84*, 346; *Angew. Chem., Int. Ed. Engl.* **1977**, *16*, 333.
(12) Herberich, G. E.; Hessner, B.; Huttner, G.; Zsolnai, L. *Angew. Chem.* **1981**, *93*, 471.
(13) Siebert, W.; Bochmann, M. *Angew. Chem.* **1977**, *89*, 483; *Angew. Chem., Int. Ed. Engl.* **1977**, *16*, 468. Siebert, W.; Edwin, J.; Bochmann, M.; Krüger, C.; Tsay, Y.-H. *Z. Naturforsch., B* **1978**, *33B*, 1410.
(14) Siebert, W.; Edwin, J.; Bochmann, M. *Angew. Chem.* **1978**, *90*, 917; *Angew. Chem., Int. Ed. Engl.* **1978**, *17*, 868.
(15) Siebert, W.; Bochmann, M. *Angew. Chem.* **1977**, *89*, 895; *Angew. Chem., Int. Ed. Engl.* **1977**, *16*, 857.

Scheme I

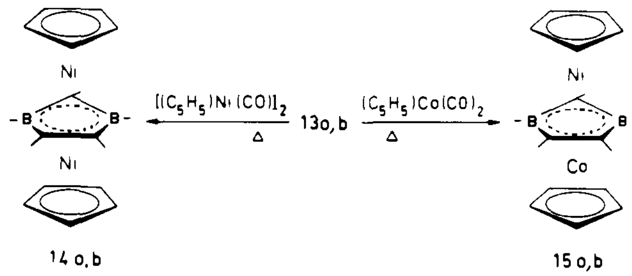

Scheme II

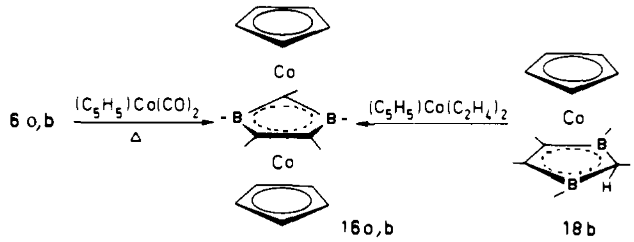

Scheme III

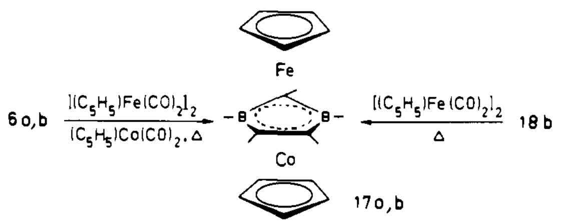

as a residue, which was identified as the quadruple-decker sandwich **20b**.

The paramagnetic dicobalt species **16a,b** are formed when the ligands **6a,b** are heated with $(C_5H_5)Co(CO)_2$ (Scheme II). Because of the insertion of the released carbon monoxide into the B–C bonds of **6a,b**,[16] the yields of **16a,b** are low (10–20%). The best synthesis (54% yield) was found to be the reaction between the new sandwich **18b**[17] and $(C_5H_5)Co(C_2H_4)_2$ in petroleum ether at 40 °C, which yielded yellow-green **16b** with 31 VE. Attempts to obtain **16b** from **18b** and $(C_5H_5)Co(CO)_2$ in mesitylene at 170 °C surprisingly yielded the brown 43 VE quadruple-decker sandwich $[(C_5H_5)Co(C_2B_2C)]_2Co$ (74%).[18]

The green, air-stable complexes **17a,b** are the 30 VE triple-deckers of this series. They can be obtained in low yield when the ligands **6a,b** and a mixture of $(C_5H_5)Co(CO)_2$ and $[(C_5H_5)Fe(CO)_2]_2$ are heated in mesitylene at 160 °C[15] (Scheme III). The assumption that the 18 VE sandwich **18** is formed in the first step[17] and then stacked with the d^7 complex fragment $(C_5H_5)Fe$ was proven by the reaction of **18b** with $[(C_5H_5)Fe(CO)_2]_2$ to form **17b** in 24% yield. As a byproduct the CoCo triple-decker **16b** is isolated. Its separation from **17b** is affected by column chromatography on silica gel with *n*-hexane. Two other routes have been studied to find a better synthesis for **17b**: the stacking of **18b** with $(C_5H_5)Fe(C_8H_{12})$ resulted in 28% yield, and the reaction of the sandwich anion $\mathbf{18b}^-$, obtained from **18b** and potassium in tetrahydrofuran,[19] with $(C_5H_5)Fe(CO)_2I$ yielded **17b** (4%) in addition to **18b** (50%), **16b** (15%), and $[(C_5H_5)Fe(CO)_2]_2$ (86%). These products are an indication that a complex reaction took place. When the NiCo triple-decker **15b** was reduced with excess of potassium in ether and an excess of $FeCl_2 \cdot 2THF$ was added

(16) Edwin, J.; Siebert, W.; Krüger, C. *J. Organomet. Chem.* **1981**, *215*, 255.

(17) Siebert, W.; Edwin, J.; Pritzkow, H. *Angew. Chem.* **1982**, *94*, 147; *Angew. Chem., Int. Ed. Engl.* **1982**, *21*, 148.

(18) Siebert, W.; Edwin, J.; Wadepohl, H.; Pritzkow, H. *Angew. Chem.* **1982**, *94*, 148; *Angew. Chem., Int. Ed. Engl.* **1982**, *21*, 149.

(19) Stumpf, K. Diploma Thesis, Universität Heidelberg, 1982.

Scheme IV

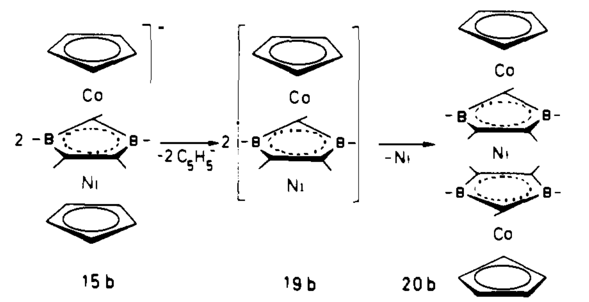

Scheme V

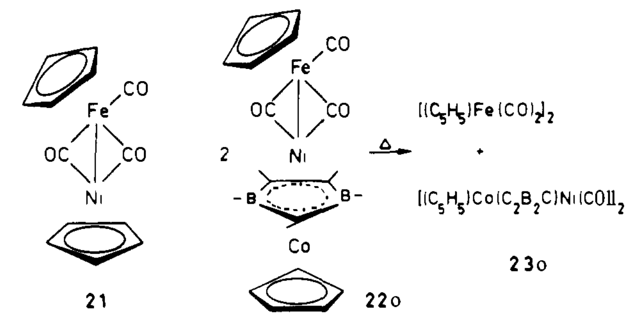

to the resulting reaction mixture, the formation of **17b** occurred in 68% yield.

Reduction of the 33 VE species **14** with potassium in THF results in the formation of the deep red diamagnetic anion[1] $\mathbf{14}^-$, which is isoelectronic with the Werner triple-decker[4] **1**. The anion is extremely air-sensitive and is oxidized to the neutral 33 VE complex. An unusual behavior of the paramagnetic nickelocene analogue **15** has been observed upon reduction with potassium in ether. The anion $\mathbf{15b}^-$ releases $C_5H_5^-$, and two of the resulting fragments **19b** form the paramagnetic 44 VE quadruple-decker sandwich **20b** in 80% yield (Scheme IV). Its constitution was proven by an X-ray structure analysis showing a trans arrangement of the coplanar diborolenyl ring.[18]

As in the case of metallocenes the triple-decker sandwiches $(C_5H_5)M(C_2B_2C)M'(C_5H_5)$ are easily oxidized with $AgBF_4$ in CH_2Cl_2 to the corresponding cations, of which $\mathbf{16}^+$ is diamagnetic. $\mathbf{14}^+$ has been also obtained from the sandwich **13b** and $AgBF_4$. The electrochemical generation of these cations and the anion $\mathbf{14}^-$ is described here:

$$(C_5H_5)M(C_2B_2C)M'(C_5H_5) \xrightarrow[-Ag]{AgBF_4} [(C_5H_5)M(C_2B_2C)M'(C_5H_5)]^+BF_4^-$$

	M	M'	VE
14^+:	Ni	Ni	32
15^+:	Ni	Co	31
16^+:	Co	Co	30
17^+:	Co	Fe	29

The close chemical relationship between nickelocene and the NiCo triple-decker sandwich **15**, both having two unpaired electrons, is demonstrated in their reactions with $Fe_2(CO)_9$. It has been long known[20] that the $Fe(CO)_3$ fragment inserts into nickelocene yielding $(C_5H_5)Fe(CO)_3Ni(C_5H_5)$ (**21**). Similarly **15a** reacts with $Fe_2(CO)_9$ in refluxing toluene to yield the trinuclear complex **22a** and several other products, which were separated by chromatography on silica gel. The 46 VE complex **22a** with one terminal and two bridging CO groups is an analogue of carbonyl-bridged **21**. It is thermally sensitive and, by a separate reaction in refluxing toluene,[21a] has been shown to undergo

(20) Tilney-Bassett, C. F. *Proc. Chem. Soc.* **1960**, 419.

Table I. Crystal Data of the Triple-Decker Sandwiches 14b, 15b, and 17b

compd	**14b**	15b	17b
space group	$P2_1/c$	$P2_1/c$	$P2_1/c$
a, Å	8.711 (1)	8.618 (3)	8.574 (2)
b, Å	17.403 (1)	17.392 (4)	17.034 (4)
c, Å	13.385 (1)	13.334 (4)	13.408 (3)
β, deg	108.53 (1)	108.13 (3)	108.33 (1)
V, Å^3	1923.8	1899.3	1858.9
Z	4	4	4
d_{calcd}, g cm^{-3}	1.362	1.378	1.402
radn	Cu Kα, 1.5418 Å	Mo Kα, 0.7107 Å	Mo Kα, 0.7107 Å
diffractometer	Nonius CAD 4	Siemens AED	Syntex R 3
θ_{max}, deg	74.7	30	30
no. of reflctns	3453	2797	3786
considered obsd	2766 (2σ)	2631 ($2.5\ \sigma$)	3417 (2σ)
R	0.078	0.103	0.041
R_w	0.095	0.088	0.056

cleavage to yield $[(C_5H_5)Fe(CO)_2]_2$ and the novel tetranuclear complex **23a** (Scheme V). This diamagnetic 58 VE CO-bridged comples is formally derived from $[(C_5H_5)Ni(CO)]_2$ by replacing the five-electron ligand C_5H_5 with the 17 VE sandwich $(C_5H_5)Co(C_2B_2C)$ radical (**18a**·, the axial hydrogen atom removed). **23a** is best obtained from **18a** and $Ni(CO)_4$ and serves as a starting compound for the construction of pentuple-decker sandwich complexes.[21b]

Other compounds from the reaction of **15a** and $Fe_2(CO)_9$ are the 30 VE triple-decker sandwich **17a** and the 31 VE triple-decker $(C_5H_5)Co(C_2B_2C)Fe(CO)_3$, formed by the fragment exchange of $(C_5H_5)Ni$ for $Fe(CO)_3$ in **15a**. A complete study of the $Fe(CO)_3$ insertion into **15a** will be published elsewhere.

Since the paramagnetic NiNi triple-decker **14b** contains two $(C_5H_5)Ni$ groups, its reaction with $Fe_2(CO)_9$ is expected to give several products. From the deep red reaction mixture through column chromatography on silica gel, five compounds were isolated. The unsymmetric 32 VE triple-decker **24b** appears to be

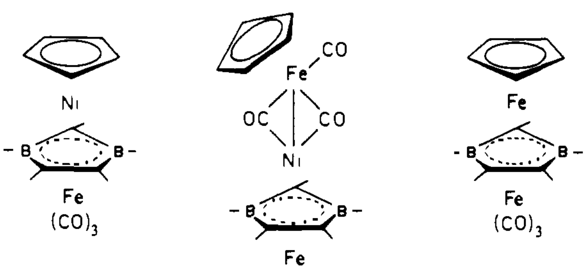

24b **25b** **26b**

the key product. In the first step one $(C_5H_5)Ni$ fragment in **14b** is replaced by $(CO)_3Fe$, thus leading to **24b**, which reacts further with $Fe_2(CO)_9$ to give the carbonyl-bridged **25b**. Elimination of Ni and CO from **25b** may lead to the diamagnetic 30 VE triple-decker $(C_5H_5)Fe(C_2B_2C)Fe(CO)_3$ (**26b**), and cleavage of **25b** yields, besides $[(C_5H_5)Fe(CO)_2]_2$, the paramagnetic 44 VE quadruple-decker complex $[(CO)_3Fe(C_2B_2C)]_2Ni$ (**27b**). This reaction sequence has also been observed in the stacking of the sandwich **13b** with the $Fe(CO)_3$ fragment.[22] Both approaches to **24b**—the $(C_5H_5)Ni$ fragment exchange for $Fe(CO)_3$ in the NiNi triple-decker **14b** and the stacking of **13b**—will be discussed in detail elsewhere. It is of interest that the 30 and 31 VE triple-decker sandwiches **17a** and **16a** do not react with $Fe_2(CO)_9$ to yield the corresponding triple-deckers by an exchange of the $(C_5H_5)Co$ fragment for $Fe(CO)_3$. However, a replacement of one C_5H_5 ligand by two CO groups in the reaction of **16a** with $Mn_2(CO)_{10}$ does take place. The air-sensitive, diamagnetic

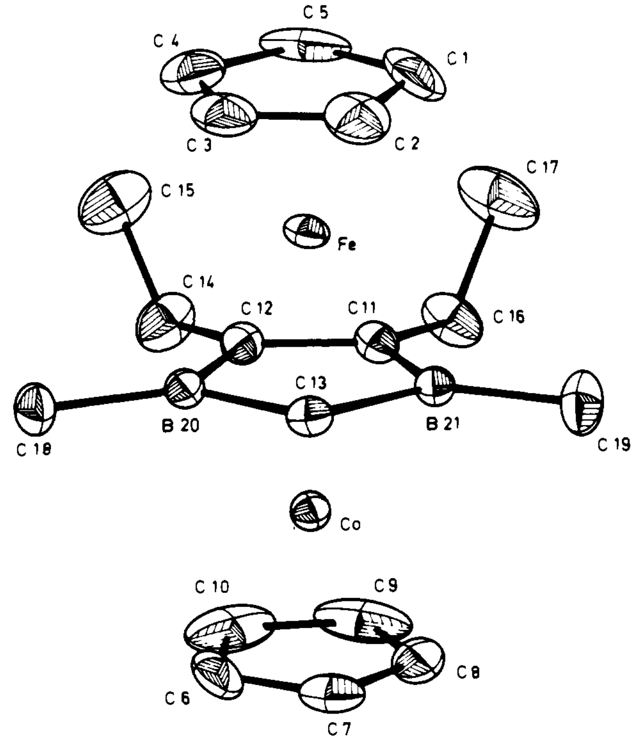

Figure 1. ORTEP drawing of the triple-decker sandwich (η^5-cyclopentadienyl)cobalt-(μ-4,5-diethyl-1,3-dimethyl-1,3-diborolenyl)(η^5-cyclopentadienyl)iron (**17b**). The thermal ellipsoids correspond to 20% probability.

Table II. Some Distances (Å) for Compounds 14b, 15b, and 17b

	14b (M1, Ni1; M2, Ni2)	15b (M1, Ni); M2, Co)	17b (M1, Fe; M2, Co)
C11–C12	1.41 (1)	1.47 (2)	1.452 (4)
C11–B21	1.58 (1)	1.57 (2)	1.589 (5)
C12–B20	1.61 (1)	1.60 (2)	1.593 (4)
C13–B20	1.54 (1)	1.52 (2)	1.561 (5)
C13–B21	1.53 (1)	1.53 (2)	1.565 (4)
M1–C11	2.140 (7)	2.223 (10)	2.090 (3)
M1–C12	2.157 (6)	2.189 (11)	2.081 (3)
M1–C13	2.141 (6)	2.121 (11)	2.059 (3)
M1–B20	2.176 (7)	2.144 (15)	2.108 (3)
M1–B21	2.183 (8)	2.146 (15)	2.125 (4)
M2–C11	2.129 (7)	1.989 (11)	2.036 (3)
M2–C12	2.100 (6)	2.052 (12)	2.028 (3)
M2–C13	2.126 (6)	2.025 (10)	2.032 (3)
M2–B20	2.177 (7)	2.107 (14)	2.095 (3)
M2–B21	2.177 (7)	2.185 (15)	2.100 (3)
M1–C(C_5H_5)	2.11–2.13	2.11–2.15	2.028–2.044
M2–C(C_5H_5)	2.06–2.10	1.99–2.08	2.026–2.035
C–C(C_5H_5)	1.28–1.42	1.33–1.42	1.33–1.49
M1–M2	3.416	3.337	3.204
M1–[C_5H_5][a]	1.775	1.775	1.659
M2–[C_5H_5][a]	1.747	1.665	1.659
M1–[C_2B_2C][a]	1.720	1.725	1.624
M2–[C_2B_2C][a]	1.698	1.609	1.580

[a] Distances from the metal atoms to the best planes through the rings.

$(C_5H_5)Co(C_2B_2C)Co(CO)_2$ (**28a**) that is formed represents a rare type of 30 VE dinuclear species with a $Co(CO)_2$ moiety.

X-ray Structure Analyses. Crystal data and details of the structure determination of **14b**, **15b**, and **17b** are given in Table I. The structures were solved by the heavy-atom method[23] and refined by least-squares techniques using anisotropic temperature factors for all non-hydrogen atoms. Only some of the hydrogen atoms could be located from difference Fourier maps. Therefore,

(21) (a) M. C. Whitley, W. Siebert, unpublished results, 1981. (b) Whiteley, M. C.; Pritzkow, H.; Zenneck, U.; Siebert, W. *Angew. Chem.* **1982**, *94*, 464; *Angew. Chem., Int. Ed. Engl.* **1982**, *21*, 465.
(22) J. Edwin, W. Siebert, unpublished results, 1981.

(23) Brauer, D. J.; Krüger, C.; *Organometallics* **1982**, *1*, 204; *Inorg. Chem.* **1975**, *14*, 3053.

Table III. Atomic Coordinates for **14b**

atom	x	y	z
Ni1	0.3744 (1)	0.3322 (1)	0.7811 (1)
Ni2	0.1941 (1)	0.5036 (1)	0.7994 (1)
C1	0.3620 (14)	0.2115 (4)	0.7799 (19)
C2	0.4904 (19)	0.2342 (6)	0.8685 (9)
C3	0.5981 (10)	0.2722 (5)	0.8369 (9)
C4	0.5526 (15)	0.2739 (5)	0.7344 (10)
C5	0.4121 (17)	0.2363 (7)	0.6944 (9)
C6	0.2356 (12)	0.6191 (5)	0.8428 (14)
C7	0.1578 (10)	0.5880 (6)	0.9020 (7)
C8	0.0133 (14)	0.5636 (5)	0.8373 (16)
C9	−0.0028 (20)	0.5759 (9)	0.7405 (14)
C10	0.1369 (27)	0.6137 (7)	0.7437 (14)
C11	0.1534 (7)	0.3954 (3)	0.7215 (4)
C12	0.2766 (7)	0.4360 (3)	0.6969 (4)
C13	0.3630 (7)	0.4215 (3)	0.8885 (4)
C14	0.2667 (11)	0.4608 (5)	0.5887 (6)
C15	0.3526 (15)	0.4221 (8)	0.5321 (8)
C16	−0.0065 (12)	0.3755 (6)	0.6398 (7)
C17	−0.0410 (19)	0.3061 (9)	0.6074 (11)
C18	0.5863 (9)	0.4970 (4)	0.8098 (6)
C19	0.0894 (10)	0.3424 (4)	0.9035 (6)
B20	0.4250 (8)	0.4546 (3)	0.8016 (6)
B21	0.1962 (8)	0.3835 (3)	0.8444 (5)

Table IV. Atomic Coordinates for **15b**

atom	x	y	z
Ni	0.37570 (16)	0.33637 (8)	0.78333 (12)
Co	0.20087 (16)	0.50474 (9)	0.80174 (12)
C1	0.3621 (20)	0.2151 (8)	0.7824 (20)
C2	0.4834 (19)	0.2380 (9)	0.8724 (14)
C3	0.5993 (16)	0.2725 (8)	0.8419 (14)
C4	0.5549 (20)	0.2785 (9)	0.7314 (15)
C5	0.4062 (18)	0.2387 (8)	0.6928 (14)
C6	0.2505 (18)	0.6148 (9)	0.8371 (17)
C7	0.1839 (16)	0.5895 (8)	0.9080 (12)
C8	0.0340 (17)	0.5569 (10)	0.8589 (15)
C9	0.0055 (20)	0.5746 (9)	0.7525 (19)
C10	0.1405 (25)	0.6118 (10)	0.7382 (15)
C11	0.1467 (12)	0.4045 (6)	0.7271 (9)
C12	0.2778 (13)	0.4415 (7)	0.6962 (9)
C13	0.3615 (12)	0.4263 (6)	0.8876 (9)
C14	0.2668 (16)	0.4654 (9)	0.5863 (10)
C15	0.3475 (17)	0.4198 (10)	0.5298 (10)
C16	−0.0184 (15)	0.3831 (7)	0.6410 (10)
C17	−0.0361 (17)	0.3078 (9)	0.6015 (13)
C18	0.5920 (12)	0.5012 (6)	0.8031 (9)
C19	0.0870 (14)	0.3472 (8)	0.9067 (10)
B20	0.4258 (14)	0.4572 (9)	0.8018 (11)
B21	0.1976 (15)	0.3843 (9)	0.8476 (11)

all of the hydrogen atoms were inserted into the calculated positions and not refined.

The assignment of the Co and Ni atoms in **15b** and of the Co and Fe atoms in **17b** was based on the comparison of the temperature factors resulting from refinements with interchanged atom factors. The resulting assignments are confirmed by the structure of the [$(C_5H_5)Co(C_2B_2C)$] unit. This unit is also found in other sandwich,[17] quadruple-decker,[24] and pentuple-decker[21b] compounds and exhibits only minor variations in the distances. In Figure 1 the triple-decker sandwich structure of the FeCo compound **17b** is illustrated, and the important interatomic distances are summarized in Table II for **14b**, **15b**, and **17b**. The three isomorphous structures consist of discrete triple-decker molecules, in which both metal atoms are η^5 bound to the central 1,3-diborolenyl ligand and to one of the terminal cyclopentadienyl rings. The accuracy of the three structure determinations is severely hampered by the rotational disorder of the cyclopentadienyl rings and by the large atomic thermal parameters. This does not permit a complete discussion and a (detailed) comparison of the structures. We hope to obtain better results on complexes containing the 1,3,4,5-tetramethyl-1,3-diborolene[25] and methylcyclopentadiene ligands.

The 1,3-diborolenyl rings are planar within ±0.01 Å (the deviations for **15b** are somewhat larger). The carbon atoms C18 and C19 attached to the borons lie in the plane of the ring, while the two other substituents on the ring, C14 and C16, are lifted out of the plane by 0.1–0.2 Å toward the metal atom M2. The planes through the cyclopentadienyl rings are parallel to the plane through the 1,3-diborolenyl ligand.

Considering the accuracy of the structure determinations, the distances (Table II) within the rings of the three structures do not exhibit large discrepancies and lie in the range found for other 1,3-diborolenyl compounds such as the sandwich **13a**, quadruple-decker sandwiches of the type **20b**,[18,24] and a pentuple-decker sandwich obtained from **23a** and **6b**.[21b] The angles in the μ-C_3B_2 rings of **14b**, **15b**, and **17b** have the following values (deg): C13–B20–C12, 102; B20–C13–B21, 113; B21–C11–C12, 111; C13–B21–C19, 130; C19–B21–C11, 128; B21–C11–C16, 125.

Changing the metal atoms has a distinct effect on the bonding between the rings. In **15b** and **17b** the diborolenyl ligand lies closer to the cobalt atom than to nickel or iron, respectively. This is in agreement with the distances (Å) found in 1,3-diborolenyl compounds from the "best" plane to the metal atom Co–(CB_2C_2), 1.56–1.60; Ni–(CB_2C_2), 1.69–1.75; Fe–(CB_2C_2), 1.70.

(24) H. Pritzkow, W. Swiridoff, W. Siebert, J. Weiss, unpublished results, 1981.

(25) U. Ender, W. Siebert, unpublished results, 1982.

Table V. Atomic Coordinates for **17b**

atom	x	y	z
Fe	0.37055 (5)	0.33934 (2)	0.78269 (3)
Co	0.20954 (4)	0.50661 (2)	0.79926 (3)
C1	0.3430 (6)	0.2212 (2)	0.7849 (6)
C2	0.4774 (7)	0.2454 (2)	0.8735 (4)
C3	0.5889 (5)	0.2808 (2)	0.8370 (4)
C4	0.5388 (7)	0.2822 (3)	0.7302 (5)
C5	0.3898 (8)	0.2445 (3)	0.6949 (5)
C6	0.2651 (6)	0.6200 (2)	0.8414 (6)
C7	0.1887 (6)	0.5890 (2)	0.9043 (4)
C8	0.0387 (6)	0.5643 (3)	0.8478 (6)
C9	0.0117 (8)	0.5780 (4)	0.7464 (6)
C10	0.1637 (13)	0.6163 (3)	0.7386 (6)
C11	0.1518 (3)	0.4023 (2)	0.7222 (2)
C12	0.2854 (3)	0.4411 (2)	0.6969 (2)
C13	0.3701 (3)	0.4269 (2)	0.8884 (2)
C14	0.2750 (6)	0.4695 (3)	0.5873 (3)
C15	0.3499 (9)	0.4174 (4)	0.5264 (4)
C16	−0.0169 (5)	0.3859 (2)	0.6433 (4)
C17	−0.0427 (8)	0.3052 (3)	0.6001 (7)
C18	0.6014 (4)	0.5034 (2)	0.8065 (4)
C19	0.0810 (5)	0.3527 (3)	0.9062 (4)
B20	0.4354 (4)	0.4591 (2)	0.8000 (3)
B21	0.1946 (4)	0.3898 (2)	0.8453 (3)

In **14b** the distance from the bridging ring to Ni2 (1.698 Å) is slightly shorter than to Ni1 (1.720 Å), and this is reflected in all of the corresponding Ni–C and Ni–B bond lengths. For most of the bonds these differences are not significant. The metal–metal distances decrease from 3.41 via 3.33 to 3.20 Å in going from **14b** to **15b** to **17b**. This indicates a stronger bonding in the triple-decker **17b** than in **15b** and **14b**, which is in line with theoretical arguments.

Atomic coordinates for **14b**, **15b**, and **17b** are given in Tables III–V, respectively.

Electronic Structure of μ-1,3-Diborolenyl Triple-Deckers. One-electron calculations of the extended Hückel (EH) type on $(C_5H_5)M(C_5H_5)M(C_5H_5)$ complexes led to simple splitting patterns for the frontier orbitals in triple-decker systems.[6] Two types of stable closed-shell species with a singlet ground state have been predicted: complexes with 30 valence electrons (VE) in which only the $3d_{z^2}$, $3d_{x^2-y^2}$ and $3d_{xy}$ AO's at the 3d centers are occupied, and 34 VE systems in which four additional electrons are filled into nonbonding or slightly antibonding MO's with large $3d_{xz}$ and $3d_{yz}$ amplitudes. However, additional difficulties are encountered in triple-decker complexes with two different metal atoms and with heterocyclic ligands. On the one hand the symmetry of the

Table VI. Orbital Energies (ϵ_i), MO Type, and Composition of the 17 Highest Occupied Orbitals of the FeCo Complex **17b** according to an INDO Calculation[a]

MO	Γ_i^+	MO type	ϵ_i, eV	Co, %	Fe, %	Cp_{Co}, %	Cp_{Fe}, %	C_3B_2, %
63	37a'	$C_3B_2(\pi)$	−8.91	2.4	3.1	9.5	16.3	68.7
62	26a''	$C_3B_2(\pi)$, $Cp_{Co}(\pi)$, Co $3d_{yz}$	−9.11	13.1	4.1	31.0	4.1	47.7
61	36a'	$C_3B_2(\pi)$, $Cp_{Co}(\pi)$, $Cp_{Fe}(\pi)$	−9.99	1.9	2.2	22.2	12.9	60.8
60	25a''	$C_3B_2(\sigma)$, $Cp_{Fe}(\pi)$	−10.23	0.5	1.9	7.8	19.5	70.3
59	24a''	$C_3B_2(\sigma)$, Fe $3d_{xy}$	−10.41	3.1	28.8	2.6	6.9	58.6
58	35a'	$C_3B_2(\sigma)$, Fe $3d_{z^2}$, $Cp_{Fe}(\pi)$	−10.44	2.2	31.0	6.8	21.3	38.7
57	34a'	Fe $3d_{z^2}$, $C_3B_2(\sigma)$	−10.59	1.0	68.7	3.3	4.7	22.3
56	33a'	Fe $3d_{x^2-y^2}$, $Cp_{Fe}(\pi)$, $C_3B_2(\sigma)$	−10.92	2.6	36.9	6.5	32.3	21.7
55	23a''	$Cp_{Fe}(\pi)$, $C_3B_2(\sigma)$, Fe $3d_{xz}$	−11.18	5.2	19.2	15.3	38.6	21.7
54	22a''	Fe $3d_{xy}$, $C_3B_2(\sigma)$, $Cp_{Fe}(\pi)$	−11.35	5.4	41.4	10.2	20.3	23.0
53	32a'	Fe $3d_{x^2-y^2}$, $C_3B_2(\sigma)$, $Cp_{Fe}(\pi)$	−11.42	2.0	39.7	1.1	11.3	45.9
52	21a''	Fe $3d_{xy}$, $Cp_{Co}(\pi)$, $C_3B_2(\sigma)$, $Cp_{Fe}(\pi)$	−11.43	13.4	25.8	22.4	13.5	24.9
51	21a'	Co $3d_{z^2}$, $C_3B_2(\sigma)$, $Cp_{Co}(\pi)$	−11.85	36.1	3.3	19.0	7.8	33.8
50	30a'	Co $3d_{z^2}$, $Cp_{Co}(\pi)$, $C_3B_2(\pi)$	−11.91	56.9	1.9	26.6	1.6	13.0
49	29a'	$C_3B_2(\sigma)$, Co $3d_{z^2}$, $Cp_{Co}(\pi)$	−12.05	26.0	0.9	14.3	8.5	50.3
48	20a''	Co $3d_{xy}$	−12.39	88.7	0.6	3.1	0.6	7.0
47	28a'	Co $3d_{x^2-y^2}$	−12.39	89.3	0.6	3.0	0.6	6.5

[a] The irreducible representations (Γ_i) correspond to the configuration of the valence electrons. The mirror plane corresponds to the x,z plane. This orientation also holds in the case of all other MO calculations.

complex is destroyed, and thus arguments based on the linear combination of equivalent fragment orbitals are no longer valid. On the other hand the basis energies of the ligand functions (occupied and virtual orbitals) are dramatically modified due to the heteroatoms in the rings.

SCF calculations of the INDO type[26] on a variety of triple-decker systems with different 3d centers as well as a large number of ligands with heteroatoms have shown that theoretical models beyond the one-electron description are necessary to rationalize the electronic structure of these complicated dinuclear complexes with sufficient accuracy.[27,28] It has been demonstrated that correlation effects, which have their origin in strongly localized wave functions and in small energy gaps between the occupied and virtual MO's, are very important for the description of the ground-state wave function. Thus, for some triple-decker complexes simple MO diagrams can only be used as a very rough approximation to rationalize their electronic structure.

In the present work we want to discuss the electronic structure of some μ-1,3-diborolenyl triple-decker species in the framework of an improved INDO Hamiltonian (see recent studies on polydecker compounds[27,28]). We have selected those systems where the Hartree–Fock (HF) method yields a sufficient approximation of the ground state. The geometrical parameters used for the calculations correspond to the X-ray data presented in this contribution.

The molecular orbitals in the outer valence region of the FeCo complex **17b** are summarized in Table VI; in addition the type as well as the composition of the MO's are displayed. It is seen that the 17 highest occupied valence orbitals can be divided into four classes. The five highest MO's are π or σ linear combinations, predominantly localized at the central diborolenyl (C_3B_2) ring with smaller contributions from the two terminal cyclopentadienyl (Cp) rings. The second class of MO's has large AO amplitudes at the iron center ($3d_{z^2}$, $3d_{x^2-y^2}$, and $3d_{xy}$). A strong coupling to the central ring (π and σ MO's) is predicted by the computational procedure. On the other hand it is seen that the Co 3d admixtures in complex orbitals with significant 3d iron character are negligibly small. The same is found in the MO's 50, 48, and 47, which are mainly localized on the Co side (class III). In these linear combinations only spurious iron admixtures are encountered. Compared to the coupling of the "Fe 3d" MO's, the coupling between the Co 3d AO's and the fragment orbitals of the ligands is dramatically reduced. It is a common feature of all triple-decker compounds with two different 3d centers that the MO wave functions are strongly localized at a single transition-metal center. This suggests that the coupling between the 3d atoms, in the case

Table VII. AO Populations at the Transition-Metal Centers for the FeCo Complexes 17b and **17b**$^+$ according to an INDO Calculation

	Co		Fe	
	charge density	spin density	charge density	spin density
	FeCo (17b) AO			
4s	0.0646		0.0858	
$4p_x$	0.0319		0.0457	
$4p_y$	0.0312		0.0453	
$4p_z$	0.0485		0.0610	
$3d_{z^2}$	1.9940		1.9858	
$3d_{xz}$	0.8521		0.7877	
$3d_{yz}$	1.3077		0.7787	
$3d_{x^2-y^2}$	1.9438		1.8285	
$3d_{xy}$	1.9440		1.8256	
	$FeCo^+$ (**17b**$^+$)			
4s	0.0649	−0.0006	0.0861	0.0015
$4p_x$	0.0317	−0.0004	0.0465	0.0006
$4p_y$	0.0310	−0.0005	0.0459	0.0006
$4p_z$	0.0484	−0.0003	0.0613	0.0006
$3d_{z^2}$	1.9946	−0.0005	1.0210	0.9721
$3d_{xz}$	0.9971	−0.4321	1.0843	0.2073
$3d_{yz}$	1.1254	−0.6225	1.1468	0.3931
$3d_{x^2-y^2}$	1.9508	−0.0076	1.8897	0.0221
$3d_{xy}$	1.9514	−0.0073	1.8911	0.0191

Table VIII. AO Populations at the Transition-Metal Centers for the NiCo Complex **15a** according to an INDO Calculation

	Ni		Co	
	charge density	spin density	charge density	spin density
	NiCo (15a) AO			
4s	0.0486	0.0002	0.0644	0.0007
$4p_x$	0.0233	−0.0002	0.0321	0.0005
$4p_y$	0.0227	−0.0002	0.0308	0.0005
$4p_z$	0.0401	0.0002	0.0480	0.0005
$3d_{z^2}$	1.9969	0.0003	1.9926	0.0010
$3d_{xz}$	1.2059	0.7632	1.0567	0.6189
$3d_{yz}$	1.6821	0.2716	1.1138	0.7172
$3d_{x^2-y^2}$	1.9727	0.0041	1.9372	0.0159
$3d_{xy}$	1.9740	0.0036	1.9387	0.0144

of different basis energies, is negligible. The fourth class of frontier orbitals in **17b** consists of MO's with LCAO amplitudes predominantly localized at the terminal Cp rings.

The populations[29] of the AO's of the transition-metal centers in the FeCo complex are shown in Table VII. The population of $3d_{xz}$ and $3d_{yz}$ on the iron atom are of comparable magnitude.

(26) Böhm, M. C.; Gleiter, R. *Theor. Chim. Acta* **1981**, *59*, 127.
(27) Böhm, M. C. *Ber. Bunsenges. Phys. Chem.* **1981**, *85*, 755.
(28) Böhm, M. C. *Chem. Phys.* **1981**, *60*, 277.

(29) Mulliken, R. S. *J. Chem. Phys.* **1955**, *23*, 1833, 2343.

Table IX. ^1H and ^{11}B NMR Data of Diamagnetic and Paramagnetic Triple-Decker Complexes 14–17

		$C-C_2H_5$			B–R				
compd	C_5H_5	α	β	C–R'	α	β	^{11}B, δ	solv	remarks
14a⁺	+39.5, +22.6, −42.8, −52							$CDCl_3$	*a*
14a	−52.69	−10.19	+8.27	−6.99	−43.08	+7.83	+1874	THF-d_8	ref 1
14a⁻	+4.81	+1.72	+1.13	+1.04	+1.21	+1.33	+7	THF-d_8	
14b	−47.72	−13.10	+8.75	+7.40	−57.31			THF-d_8	
14b⁻	+4.83	+1.70	+1.16	+0.45	+0.35			THF-d_8	
14b/14b⁻	−21.14	−5.77	+4.90	+3.95	−28.16			THF-d_8	mixture 1:1
15a⁺	+9.6, +4.60, +2.80, +1.47, −5.36, −55							$CDCl_3$	*a*
15a	+15.4, +14.23, +5.14, −13.9, −20.8, −24.5, −26.7							CS_2	*a*
15b	+94.0, +13.7, −17.1, −54.4							C_6D_6	*a*
16a⁺	+4.95	+2.82	+1.44	+2.10	+2.08	+1.60	+19.5	$CDCl_3$	
16a	+9.6, +4.4, −7.8, −17.1, −20.1, −59.0							C_6D_6	*a*
17a	+3.61 +3.55	+2.6	+1.55	+2.07	+2.0(m)		+19.6	C_6D_6	
17b⁺	+25.6, +20.2, +17.9, +11.8, −10.0, −23.6							CD_2Cl_2	*a*
17b	+3.70 +3.51	+2.7 +2.5	+1.61	+2.71	+1.79		+18.0	C_6D_6	

a Consult text.

An inequivalence in the population of $3d_{xz}$ and $3d_{yz}$ is predicted for the Co center. The antibonding interaction with the central ligand is minimized if $3d_{yz}$ is highly populated due to the "vacant" π functions of the boron centers. Similar effects have also been detected in mononuclear metallocenes with B-containing ligands.[30]

In the NiCo complex 32 VE are encountered, which leads to a triplet ground state. In analogy to the FeCo system strongly localized MO's with large transition-metal amplitudes are predicted. The center of gravity of the Ni 3d linear combinations is found at about −14 eV. The Co 3d orbitals are shifted about 1.5 eV to lower energies. The charge and spin densities of the 3d centers of the NiCo derivative are given in Table VIII. Once again the populations of $3d_{xz}$ and $3d_{yz}$ at the 3d center with the smaller atomic number (Co) are comparable while a pronounced difference in the occupation of both AO's is diagnosed for Ni. Furthermore the INDO results in Table VIII indicate that the two unpaired electrons (contributions from the 3d centers) are found in the $3d_{xz}$ and $3d_{yz}$ AO's. Spin polarization effects in the lower 3d sets ($3d_{z^2}$, $3d_{x^2-y^2}$, and $3d_{xy}$) are negligible. The α-spin surplus at Co is compensated by the enhanced β-spin density of the diborolenyl fragment, while the spin density of the terminal ligands is small compared to the spin density of the $Ni(C_3B_2)Co$ fragment. The same behavior is also predicted for the other open-shell species in the triple-decker series.

In Figure 2 the Wiberg bond indices[31] for $NiCo^-$, for a representative set of 30 VE compounds (FeCo, $CoCo^+$), and for 32 VE systems (NiCo, $CoCo^-$, $NiNi^+$) with triplet ground states are summarized. Obviously the magnitude of the covalent coupling between the 3d center and the ligands is reduced when the number of 3d electrons at the transition-metal center is increased. In the FeCo complex **17b** the strongest interaction between the 3d center and the ligands is predicted for Fe and cyclopentadienyl.

The corresponding CoCp indices amount to only two-thirds of the FeCp indices. With respect to the central diborolenyl ligand a predominance of the $Co(C_3B_2)$ interaction is found. The CoCp indices in $CoCo^+$ are larger than the CoCp bond indices in FeCo and reflect the pronounced charge redistribution due to the different 3d centers.

The covalent interaction is dramatically reduced in the 32 VE species. In the neutral NiCo complex the aforementioned polarization of the electron distribution is clearly seen. The Wiberg indices between Ni and the ligands are significantly smaller than the bond indices with respect to the Co atom. Of course, the weakest covalent interaction is found in $NiNi^+$.

Physical Properties of Triple-Deckers

Spectroscopic Studies: NMR and ESR Data. Magnetic resonance measurements were made on several compounds and ions

(30) Böhm, M. C.; Eckert-Maksić, Gleiter, R.; Herberich, G. E.; Hessner, B. *Chem. Ber.* **1982**, *115*, 754.

(31) Wiberg, K. B. *Tetrahedron* **1968**, *24*, 1083.

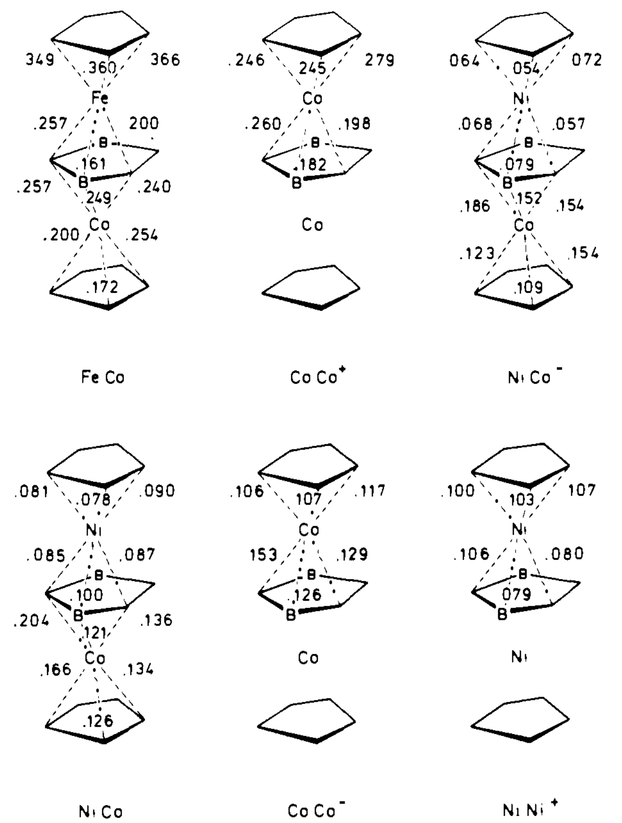

Figure 2. Wiberg bond indices of the 30 VE species FeCo and $CoCo^+$ as well as of the 32 VE triple-decker complexes NiCo, $CoCo^-$, $NiNi^+$, and $NiCo^-$ (33 VE) according to the INDO Hamiltonian.

derived from **14–17**. Table IX summarizes the chemical shifts of the para- and diamagnetic compounds. The assignment of the signals for the diamagnetic species **14⁻**, **16⁺**, and **17** is straightforward. Since the methylene protons of the $C-C_2H_5$ groups in **14⁻** and **16⁺** appear as quartets, they are magnetically equivalent and indicate the arrangement of the triple-decker. (In the sandwich complexes **13** and **18** the protons of the ethyl groups appear as ABX_3 multiplets.)

The paramagnetic triple-decker sandwich complexes **14–16** as well as the paramagnetic triple-decker cations **14⁺**, **15⁺**, and **17⁺** give NMR spectra. Of the paramagnetic compounds a complete NMR analysis[1] has been carried out only for **14a**. As shown in Table IX, the ^1H and ^{11}B signals cover spectral ranges of about 60 and 1900 ppm, respectively. ^{13}C signals[1] appear within 1000 ppm. The assignment of the signals is assured by selective decoupling. A series of ^1H NMR spectra was obtained of mixtures

Table X. Parameters Derived from Electron Spin Resonance Spectra of Radical Ions of Triple-Decker Sandwich Compounds

radical	method of production	g_1	g_2	g_3	a_1[a]	a_2	a_3
$[CpFe(C_2B_2C)CoCp]^+$ (**17a⁺**)	electrolysis	2.11			ca. 50		
$[CpFe(C_2B_2C)CoCp]^-$ (**17a⁻**)	metal reduction	2.21	2.01	1.78	135		
$[CpNi(C_2B_2C)CoCp]^+$ (**15a⁺**)	electrolysis	2.15	2.01	1.95	27		
$[CpNi(C_2B_2C)CoCp]^-$ (**15a⁻**)	metal reduction		2.02		no hyperfine splitting; $\Delta H = 33$ G		

[a] Cobalt hyperfine splitting in gauss.

Table XI. Mössbauer Effect Data for the Triple-Decker Sandwich FeCo and Its Cation $FeCo^+$

	χ^2, ch	*T*, K	E^Q, mm·s^{-1}	σ_{IS}, mm·s^{-1} (^{57}CoRh)	NNP[b]	ampl 1 / ampl 2	Γ, mm·s^{-1}
FeCo (**17b**)	1.7	4.2	2.57 (3)	0.30 (1)		1.004	0.26 (1)
	1.2	80	2.50 (3)	0.35	0.72	0.986	0.30 (1)
	1.04	200	2.48	0.314	0.684	0.939	0.258
	0.90	295	2.45	0.26	0.63	0.884	0.24
	1.01[a]	<300	2.41	0.254	0.624	0.860	0.255
$FeCo^+$ (**17b⁺**)	1.13	4.2	0.279	0.251		1.0	0.291
	1.05	80	0.267	0.306	0.676	1.04	0.30
		295	0.246	0.165	0.535		0.26
Cp_2Fe			2.40		0.790		
$Cp_2Fe^+BF_4^-$					0.83		

[a] Absorber ∠40° to the direction of the γ beam. [b] σ_{IS} relative to σ_{IS} for $Na_2[Fe(CN)_5NO]\cdot H_2O$.

of **14** with its anion, prepared through the partial reduction of **14** with potassium. The electron transfer between the species is fast, so that average NMR signals are observed. The dependence of the chemical shifts (δ) on the molar fraction of the couple **14b**/**14b⁻** has been published elsewhere.[8b] Straight lines are obtained when δ is plotted against the molar fraction of **14b**. An example is given in Table IX. The assignment of all of the signals from **14b** arises from the known resonance positions of diamagnetic **14b⁻**, double resonance experiments, and integration of the signals. Up to now we have been able to get full assignments only for paramagnetic **14a** and **14b**. Unfortunately we do not know the *g* anisotropy of these radicals because we failed to obtain the ESR spectra. Therefore, a conversion of the paramagnetic shifts to hyperfine coupling constants is not possible. However, we get a clear pattern of the signs of the ^{1}H hyperfine coupling constants of the central ring, which are positive for ring hydrogens, negative for α-positions, and again positive for β-positions. The cyclopentadienyl hydrogens show a negative hyperfine coupling constant. The same alternation of signs seems to be realized for **15** and **16**. This is shown by the differences between the ^{1}H NMR spectra of **15a**/**15b** and **16a** (Table IX). The similarity of **14**–**16** may be the result of the same type of MO playing the role of the HOMO in all three cases.

The rapid relaxation effects, which result in sharp-line NMR spectra, made the ESR spectra of the paramagnetic triple-deckers more difficult to obtain. No spectrum for dilute glasses of the dicobalt compound **16a** was observed even at 77 K. The spectra of other compounds with mixed metals were sharp at liquid nitrogen temperatures, although severe line broadening was usually evident at temperatures above 150 K. This behavior can be rationalized on the basis of slower spin–lattice relaxation in the mixed-metal compounds, due to a less efficient coupling of the excited and the ground electronic states of these compounds of lower symmetry.

The most complete ESR data were obtained for the ions derived from the FeCo species **17a**. Alkali metal reduction of **17a** in THF gave solutions of **17a⁻**, which when frozen at 77 K, gave a rhombic **g** tensor ESR spectrum (Figure 3). Five of the eight expected cobalt hyperfine lines along the low-field component were resolved. The ESR data are summarized in Table X. The radical cation of **17a** was generated by the electrolysis of a solution of the neutral compound in CH_3CN at a platinum electrode. The frozen solution gave a spectrum of approximately axial symmetry with poorly resolved cobalt hyperfine splittings of ca. 50 G on the low-field side of the spectrum. There is a very large difference in the magnitude of the low-field cobalt splitting between **17a⁻** and **17a⁺**,

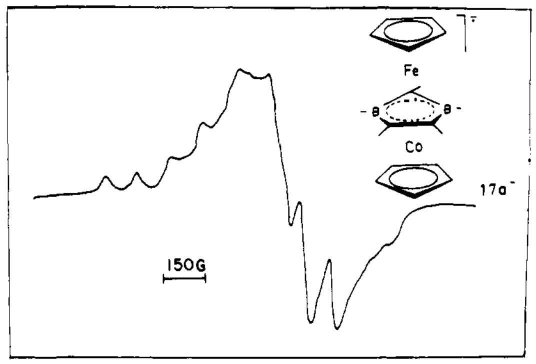

Figure 3. ESR spectrum of the FeCo monoanion (**17a⁻**) at 77 K generated via Na/K metal reduction in THF.

namely 135 vs. 50 G. Qualitatively this could be used to suggest a larger cobalt contribution to the HOMO rather than to the LUMO of **17a**. But any attempt to quantify the electronic structure of the radical ions requires data of higher quality, preferably on single crystals, in which it is hoped that the high-field cobalt splitting can be resolved.

Similar observations were made for the radical ions derived from the CoNi compound **15a**. In this case, however, the assignment of the spectrum of the anion is less certain. Attempts to produce the anion electrolytically were unsuccessful due to the strong tendency of **15a⁻** to revert to **15a** in dilute solutions, even under drybox conditions. The alkali metal reduction of THF solutions of **15a** gave the characteristic deep green color of the anion but yielded an ESR spectrum much different from those of the others in the series. A single line with $g = 2.02$ and a line width of 33 G was obtained at 77 K. This line disappeared when the solution was thawed and refrozen or exposed to oxygen. If this is truly the spectrum of **15a⁻**, there must be little involvement of cobalt in the half-occupied orbital.

A more definitive spectrum was obtained for **15a⁺** through the electrolysis of **15a** in CH_3CN at +0.30 V. The frozen solutions gave very broad lines at 150 K, but sharp lines at 77 K, and allowed the observation of the rhombic **g** tensor spectrum displayed in Figure 4. The only cobalt hyperfine splitting observed, along the low-field direction, was very small (27 G).

One trend may be noted concerning the ESR data. In each case the highest value of *a* (Co) is along the low-field *g* component.

Mössbauer Effect and Magnetic Measurements. The ^{57}Fe Mössbauer spectra of **17b** (FeCo) and **17b⁺** $FeCo^+BF_4^-$ were

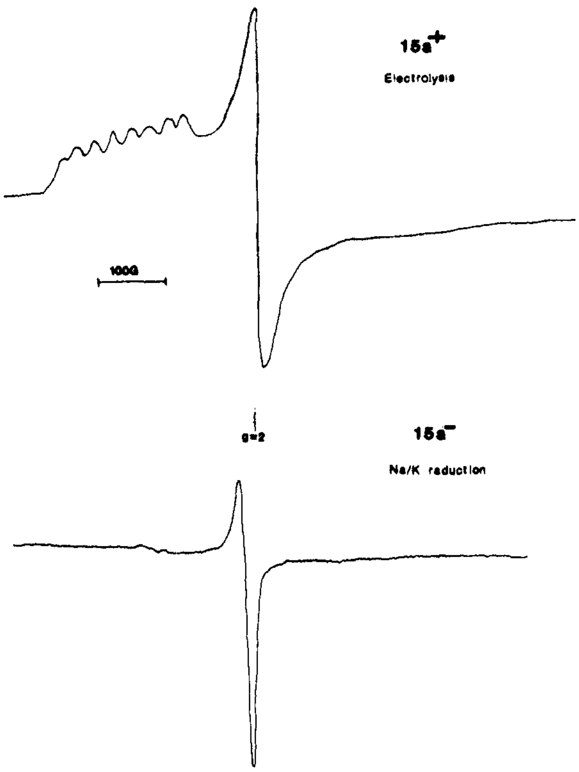

Figure 4. ESR spectra of the NiCo monoanion ($15a^-$) and monocation ($15a^+$) in THF at 77 K.

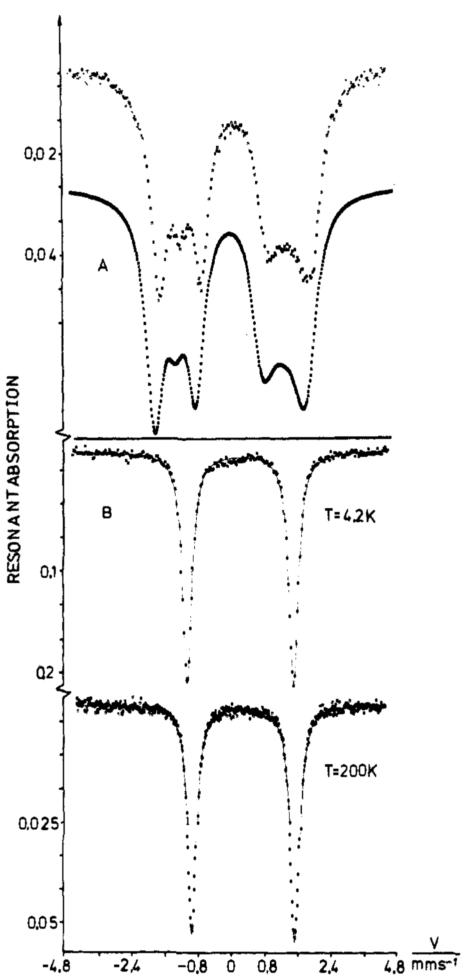

Figure 5. Mössbauer spectrum of FeCo (**17b**): (A) applying a magnetic field of 40 kG at 4.2 K; (B) asymmetric, quadrupole-split absorption.

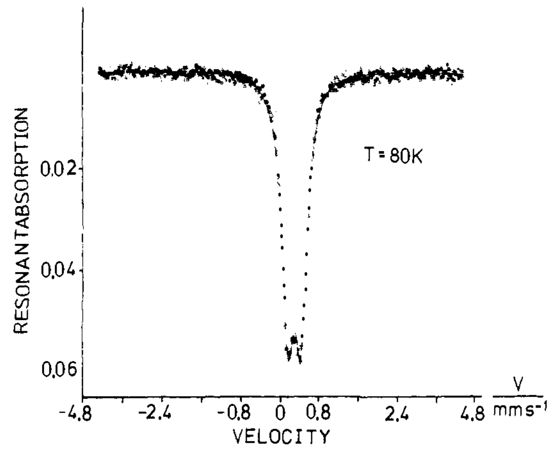

Figure 6. Mössbauer spectrum of $FeCo^+BF_4^-$ ($17b^+$) at 80 K.

analyzed by a least-squares fit program with a single Lorentzian and line widths $\Gamma_1 = \Gamma_2$. The solid lines in Figures 5 and 6 represent the computed shapes of the Lorentzian. The Mössbauer data for FeCo and $FeCo^+BF_4^-$ are summarized in Table XI. The Mössbauer spectrum of FeCo consists of a weak, temperature-dependent quadrupole splitting, ΔE^Q, in the temperature range between 4.2 and 295 K. The sign of the electric quadrupole splitting was determined by applying a magnetic field of 40 kG at 4.2 K. It was noted that the low- and high-energy components split into a triplet and a doublet, respectively (Figure 5A). A first-order perturbation theory treatment yields a ΔE^Q ($= {}^1/_2 e^2qQ = +2.5$ mm·s^{-1}) that is positive. This was also determined for ferrocene.[32] The differences in ΔE^Q and δ for Cp_2Fe and FeCo are very small, suggesting a very similar electronic structure around the iron nucleus of both compounds.

The spectra in Figure 5B show an asymmetric, quadrupole-split absorption. We note that the asymmetry increases with increasing temperature, which may be an indication that the recoil-free fraction is anisotropic (known as the Goldanskii effect). The possibility of orientation has been discounted because of the absence of an angular dependence of the spectra at $T = 295$ K. Such an asymmetry can also be the result of fluctuating electric fields, which can be produced by fluctuations in the environment of the ^{57}Fe nucleus. These relaxation effects can lead to a variety of temperature dependencies for the asymmetry of the quadrupole lines. In most cases, the opposite of that expected on the basis of a Goldanskii effect is observed.

The quadrupole splitting for FeCo is reduced to a small, but nevertheless resolved splitting, $\Delta E^Q = 0.29$ mm·s^{-1}, when FeCo is oxidized to $FeCo^+BF_4^-$ (Table XI). It is reasonable to assume that similar effects are responsible for this variation in ferrocene and in the FeCo system. The sign of ΔE^Q in ferrocene has been rationalized on the basis of crystal-field calculations and on the basis of early MO approaches. The crystal-field formalism of Matsen[33] leads to a negative sign for ΔE^Q, while the MO calculations of Dahl and Ballhausen,[34] using Watson's wave functions for iron, predicted ${}^1/_2 e^2qQ$ to be positive. In contrast to the neutral molecules, the corresponding cations Cp_2Fe^+ and $FeCo^+$ exhibit almost no splitting (Table XI). In the case of the ferricenium cation this behavior has been explained by Collins[32] to be the result of mutually cancelling contributions to the electric-field gradient tensor **q**. If the theoretical suggestions for the ferricenium ion are adopted for the $FeCo^+$ system, the very small quadrupole splitting $\Delta E^Q = 0.29$ mm·s^{-1} should have its origin in a cationic state that is similar to the $^2E_{2g}$ ground state of the Cp_2Fe^+ ion (e.g., removal of an electron out of an e_{2g} descendant in the

(32) Collins, L. L. *J. Chem. Phys.* **1965**, *42*, 1072.
(33) Matsen, F. A. *J. Am. Chem. Soc.* **1959**, *81*, 2023.
(34) Dahl, J. P.; Ballhausen, C. F. *Mat. Fys. Medd. Dan. Vid. Selsk.* **1961**, *33*, No. 5.
(35) Maki, A. H.; Berry, T. E. *J. Am. Chem. Soc.* **1965**, *87*, 4437.
(36) Henrickson, D. N.; Sohn, Y. S.; Gray, H. B. *Inorg. Chem.* **1971**, *10*, 1559.

Table XII. Magnetic Moments, μ_{eff}, at Room Temperature for Triple-Decker Complexes

complex	μ_{eff}, μ_B	valence electrons
FeCo (17b)		30
$FeCo^+BF_4^-$ (17b$^+$)	2.10 (2)	29
$Cp_2Fe^+BF_4^-$	2.44	17
CoCo (16a)	1.78 (10)	31
$NiCo^+$ (15a$^+$)	1.80 (10)	31
NiCo (15a)	2.78 (10)	32
$NiNi^+$ (14a$^+$)	2.90 (10)	32
NiNi (14a)	1.88 (10)	33

Table XIII. Cyclic Voltammetry Data[a] for Triple-Decker Compounds $CpM(C_2B_2C)M'Cp$

triple-decker	couple	$E°$,[b] V	e_p[c]	current ratio[d]	ν[e]	electrode
FeCo (17a)	+/0	−0.06	64	1.0	0.10	Hg or Pt
	0/−	−1.76	65	1.0	0.10	Hg
CoCo (16a)	2+/+	+1.74	120	0.6	0.16	Pt
	+/0	−.57	60	1.0	0.10	Hg or Pt
	0/−	−1.53	70	1.0	0.10	Hg or Pt
	−/2−	−2.56	h	h	0.10	Hg
CoNi (15a)	2+/+	+1.00	h	h	0.10	
	2+/+	+1.08	70	1.0	0.05	Pt (CH_2Cl_2)[g]
	+/0	+.06	62	1.0	0.10	Pt
	0/−[i]	−1.63	60	0.85	0.20	Pt
CoNi (15a)	0/−	−1.58	80	1.0	0.10	Pt (THF)[f]
NiNi (14a)	2+/+	+1.26	h	h	0.10	Pt
	+/0	−0.13	64	1.0	0.04	Hg or Pt
	0/−	−1.30	66	1.0	0.10	Hg or Pt

[a] Data reported for 0.1 M Bu_4NPF_6/CH_3CN solutions. [b] Volt vs. aqueous SCE; $E°$ reported for reversible systems, e (peak) for irreversible systems. [c] Separation (in mV) of cathodic and anodic peaks. [d] i_a/i_c for reductions; i_c/i_a for oxidations. [e] Scan rate in V/s. [f] THF solutions, 0.1 M Bu_4NPF_6. [g] CH_2Cl_2/0.1 M Bu_4NPF_6. [h] Irreversible. [i] Product peak oxidation at −1.48 V; slow scans.

Table XIV. dc Polarography Data[a] on Triple-Decker Compounds $CpM(C_2B_2C)M'Cp$

metals	couple	$E_{1/2}$[b]	slope[c]	I[d]
FeCo (17a)	+/0	−0.058	61	2.92
	0/−	−1.766	58	2.79
CoCo (16a)	+/0	−0.57	63	2.36
	0/−	−1.53	66	2.77
	−/2−	−2.56		
CoNi (15a)	+/0	+0.03	67	3.81
	0/−	−1.66	66	5.25
CoNi (15a)	0/− (THF)	−1.66	65	3.34[e]
NiNi (14a)	+/0	−0.13	60	2.95
	0/−	−1.31	57	2.77

[a] Electrolyte = 0.1 M Bu_4NPF_6 in CH_3CN. [b] Volt vs. aqueous SCE. [c] Slope of plot of $-E$ vs. log $[i/(i_d - i)]$ (in mV). [d] Diffusion current constant. [e] THF solution; I value for one-electron standard $Ni(1,2\text{-}C_2B_9H_{11})_2$ was 3.10 in this solvent.

triple-decker).[37] In this model the ground state of Fe is $^2E_{2g}$ $(a_{1g})^2(e_{2g})^3$ in $FeCo^+BF_4^-$. In analogy to the ferricenium cation,[35] we assume that the ground state, $^2E_{2g}$, is also split into two Kramers doublets by spin–orbit coupling and crystal fields of symmetry lower than D_5. Wave functions and energies for the lower $\psi\pm^a$ and the upper $\psi'\pm^b$ doublet have been given.[35] The magnetic susceptibility

$$\chi = \tfrac{1}{3}(\chi_\parallel + 2\chi_\perp)$$

for $FeCo^+BF_4^-$ was evaluated by considering only the two Kramers doublets[36] of the $^2E_{2g}$ ground state:

$$\chi_\parallel(\psi\pm^a) = \frac{N\mu_B^2}{kT}\left[\left(1 + \frac{2K'(1-\zeta^2)}{(1+\zeta^2)}\right)^2 + \frac{16\zeta^2K'^2kT}{(\xi^2+\delta^2)^{1/2}(1+\zeta^2)^2}\right]$$

$$\chi_\perp(\psi\pm^a) = \frac{N\mu_B^2}{kT}\,\frac{4\zeta^2}{(1+\xi^2)^2} + \frac{kT(1-\zeta^2)^2}{(1+\zeta^2)^2(\xi^2+\delta^2)^{1/2}}$$

The mixing parameter ζ, the spin–orbit coupling constant ξ, and the low-symmetry distortion parameter δ are defined in ref 35. We have used the one-electron spin–orbit constant $\xi_0 = 405$ cm^{-1} and an orbital reduction factor $K' = 0.8$ to obtain δ. In Figure 7, A and B, the solid lines represent the calculated values of the reciprocal susceptibility χ_M^{-1} and the effective magnetic moment μ_{eff} as a function of the temperature in the range 10 K $\leq T \leq$ room temperature, respectively. The best agreement between experimental and calculated values was obtained with $\delta = 650$ cm^{-1}, $\xi = -K'\xi_0 = 324$ cm^{-1}, and $\zeta = 0.62$. According to our calculations the energy splitting $2(\xi^2 + \delta^2)^{1/2}$ (the difference between the lower $\psi\pm^a$ and the upper $\psi\pm^b$ doublet) is 1450 (±40) cm^{-1}, which is obviously too large to have an appreciable population in $\psi\pm^b$. (Predicted values are 924 cm^{-1} for $Cp_2Fe^+BF_4^-$, 1300–1500 cm^{-1} for carboranyl ferricenium analogues,[35] and about 1610 cm^{-1} for $FeCo^+$ (this work).)

In comparison to Cp_2Fe^+ we conclude that the more asymmetric the environment of the Fe, the more pronounced is the change (decrease) in μ_{eff}. If the distortion is very large, the orbital contribution to the magnetic moment would be quenched, resulting in an essentially spin-only value for μ_{eff} equal to 1.73 μ_B.

On the other hand, the semiempirical INDO calculations on the FeCo cation lead to a ground state in which an electron has been removed from the Fe $3d_{z^2}$ orbital (a_{1g} combination in D_{5d}). This may be an artifact of our MO approach since the sequence of the $^2A_{1g}$ and $^3E_{2g}$ states of the ferricenium ion is exchanged.[38]

It should be mentioned, however, that the present selection of parameters (ξ_0, δ, ΔE) is only one set in a manifold of values, where the magnitude of ξ_0 and δ differ from the Cp_2Fe^+ increments. For example, we cannot rule out that the exact "δ" in $FeCo^+$ must be increased (lower symmetry) while the exact "ξ_0" must be reduced (stronger delocalization of the orbital wave function).

In Table XII the room-temperature magnetic moments of the 29–33 valence electron triple-decker complexes are listed. As predicted by MO considerations the observed magnetic moments of the species with 31 and 33 valence electrons fall into the range expected for one unpaired electron, whereas **15** and **14**$^+$ (with 32 valence electrons) exhibit magnetic moments expected for two unpaired electrons.

Electrochemistry. General Electrochemical Behavior. These compounds were investigated by direct current (dc) and phase-selective alternating current (ac) polarography, cyclic voltammetry, and controlled-potential coulometry. All the dc polarographic waves were found to be diffusion controlled by making plots of the polarographic plateau current as a function of the square root of the height of the mercury column. These plots were linear and passed through the origin of the graph. Likewise, a test for diffusion control was made in all of the cyclic voltammetry experiments by plotting the peak current as a function of the square root of the scan rate. These plots were all linear, passed through

(37) For the argumentation, the irreducible representations used are those that have been adopted in various physical studies on the unperturbed Cp_2Fe moiety: a_{1g} ($3d_{z^2}$) and e_{2g} ($3d_{x^2-y^2}/3d_{xy}$). The MO calculations presented in the foregoing section, however, have shown that this classification scheme can be only a rough approximation for the iron 3d orbitals at the iron site. Strictly speaking, the modification of the electronic structure due to the low-symmetry heteroligand is more than a weak perturbation. The D_{5d} nomenclature thus is used in the first place to link our results to the previous studies (Mössbauer, magnetic measurements) on the ferricenium ion. As a result of the reduced symmetry in the FeCo triple-decker, the e_{2g} representation of the point group D_{5d} splits into an a′ and an a″ component. Thus the following one-to-one correspondence between the two sets of irreducible representations holds:

$CpFe_2$	FeCo	3d AO
a_{1g}	a′	$3d_{z^2}$
e_{2g}	a′	$3d_{x^2-y^2}$
	a″	$3d_{xy}$

(38) Böhm, M. C.; Gleiter, R.; Delgado-Pena, F.; Cowan, D. O. *Inorg. Chem.* **1980**, *19*, 1081.

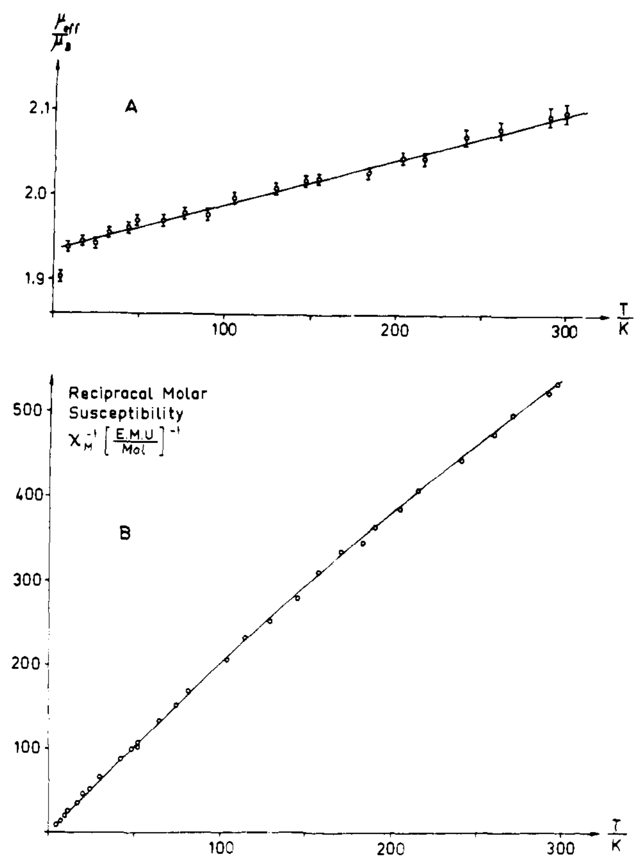

Figure 7. (A) Effective magnetic moment of $FeCo^+BF_4^-$ (**17b**$^+$) as a function of the temperature (10–300 K). (B) Reciprocal susceptibility χ_M^{-1} as a function of temperature.

the origin, and were consistent with a diffusion control of mass transport.

Cyclic voltammetry data suggest that the electron-transfer reactions are very rapid, i.e., electrochemically reversible. In support of this contention, the differences between cathodic and anodic peak potentials of a redox couple (Δe_p) were generally 60–70 mV at moderate scan rates (ca. 0.1 V/s). Specific data are given in Table XIII. With the exception of the reduction of **15a** in CH_3CN, all of the represented waves were one-electron transfers. A variety of electrochemical measurements were consistent with this interpretation. Diffusion current constants, I_d, for the couples accessible to dc polarography were in the one-electron range, as shown by a comparison of the values for the triple-decker compounds with that of a one-electron standard, $(C_5H_5)_2Co^+$, which has I_d = 3.6 in CH_3CN for the $(C_5H_5)_2Co^+/(C_5H_5)_2Co$ couple. The I_d values are found in Table XIV. Another piece of evidence in favor of one-electron transfers was derived from the shapes of the dc polarographic curves. Plots of $-E$ vs. log $[i/(i_d - i)]$ were linear with slopes of about 60 mV (Table XIV), the value expected for a reversible one-electron process. In CV measurements, besides the Δe_p values of ca. 60 mV, the one-electron nature of the redox steps was also established by the peak currents of the waves. For each compound the wave heights for reductions or oxidations were compared with the height of a one-electron standard (usually $(C_5H_5)_2Co^+$) at the same scan rate and concentration, and the peak currents were always within 5% of the value of the one-electron standard. Finally, bulk coulometry at controlled potential was employed to measure n values. Again, these values were very close to 1. Actual numbers are found in the running text.

$(C_5H_5)Fe(C_2B_2C)Co(C_5H_5)$ (17a). The FeCo triple-decker undergoes a reversible oxidation and reduction to a monocation ($E°$ = −0.06 V) and monoanion ($E°$ = −1.77 V), respectively. Bulk coulometry in CH_3CN at +0.20 V at a platinum basket (n = 1.0e$^-$) gave a stable solution of the monocation, from which a solution was withdrawn for ESR studies (vide ante). The neutral compound could be quantitatively regenerated by back-electrolysis at −0.20 V.

The monoanion of **17a** was more difficult to obtain. Repeated attempts to generate stable solutions of it by electrolysis of the neutral compound at −2.0 V under nitrogen failed due to rapid regeneration of the neutral compound. No other products were formed. This problem plagued all electrochemical attempts to form stable anionic triple-deckers, which apparently are very prone to reactions with adventitious oxygen or other impurities. Alkali metal reductions, either for preparative purposes or for preparation of ESR samples, were more successful in preparation of the anions, apparently since either much higher concentrations or more rigorous (high vacuum) conditions were employed in the nonelectrochemical approach.

The electron-transfer series for the FeCo triple-decker thus encompasses three members, from the 29-electron cation to the 31-electron anion, which we abbreviate as

$$FeCo^+ \rightleftharpoons FeCo \rightleftharpoons FeCo^-$$

$(C_5H_5)Co(C_2B_2C)Co(C_5H_5)$ (16a). This neutral 31-electron species underwent four redox processes, two reductions (−1.53 and −2.56 V) and two oxidations (−0.57 and +1.74 V). Reduction to the monoanion and oxidation to the monocation are completely reversible, so that the singly charged species are both stable. A second one-electron reduction (−2.56 V) was irreversible, and it is clear that the CoCo dianion, a 33-electron species, is highly unstable. The second oxidation, to **16a**$^{2+}$, is reversible at higher scan rates, and from our cyclic voltammetry data we estimate the lifetime of the dication to be several seconds at room temperature in CH_3CN. Thus, the electron-transfer series for the dicobalt triple-decker encompasses five species, from the 29-electron dication to the (very transient) 33-electron dianion:

$$CoCo^{2+} \rightleftharpoons CoCo^+ \rightleftharpoons CoCo \rightleftharpoons CoCo^- \rightarrow CoCo^{2-} \rightarrow ?$$

Pea-green solutions of the neutral compound in either THF or CH_3CN were electrolyzed at −0.30 V (platinum electrode) to oxidize the compound. The solution turned to the deep green of the monocation (n = 0.8e$^-$), and CV scans on the resulting solution indicated that the monocation was the only product formed. The original neutral compound could be quantitatively regenerated by reduction of the deep green solution at −0.80 V.

$(C_5H_5)Co(C_2B_2C)Ni(C_5H_5)$ (15a). This compound underwent only one reduction and two oxidations. The first oxidation, to the 31-electron cation, was reversible in CH_3CN ($E°$ = +0.03 V), THF, or CH_2Cl_2. Bulk oxidation in CH_3CN at +0.30 V at a platinum basket resulted in release of one electron (n = 0.9e$^-$) as the solution changed from the deep blue-green of the neutral compound to the chocolate brown of the cation. Reelectrolysis at −0.40 V completely regenerated the starting compound. Oxidations in dichloromethane gave more stable solutions of the cation, which tended to reduce back to the neutral compound on standing in CH_3CN. Thus, oxidation at +0.30 V released one electron (n = 0.9e$^-$) and a dc polarogram of the resulting deep brown solution had a reduction wave at $E_{1/2}$ = +0.11 V. The height of the wave was the same as the original oxidation wave, measured before electrolysis, which had a value of +0.12 V in this solvent. There was a second oxidation to a dication, which was irreversible in CH_3CN (e_{p_a} = +1.00 V) (Figure 8) but highly reversible in CH_2Cl_2.

At a scan rate of 0.10 V/s in CH_2Cl_2 a value of 0.97 was calculated for the ratio i_c/i_a, showing that the dication is stable on this time scale. We could not, however, generate stable solutions of the dication, for electrolysis at +1.2 V yielded only solutions of the monocation, showing that the dication spontaneously regenerates the singly charged species.

The reduction of the NiCo compound in THF was straightforward ($E°$ = −1.58 V, Δe_p = 80 mV at v = 0.1V/s) and was consistent with a one-electron reversible reduction to a monoanion. Coulometry at a platinum basket yielded deep green solutions of the monoanion (n = 1.0e$^-$) that were stable although very air-sensitive, so that samples for ESR were prepared by subambient-temperature (200 K) alkali metal reduction. Although our

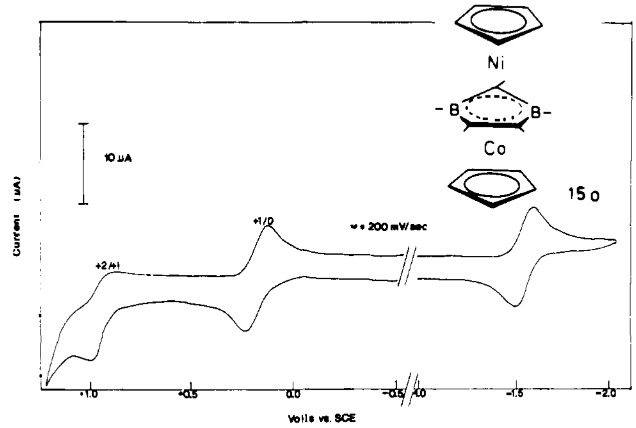

Figure 8. Cyclic voltammogram of the CoNi triple-decker at the Pt electrode in CH_3CN/Bu_4NPF_6; v = 200 mV/s.

electrochemical experiments were too short in duration to test the very long-term stability of **15a**$^-$, they do demonstrate that synthesis of the quadruple-decker **20b** from **15b**, which is a 16-h reaction in THF with alkali metal, must proceed through the monoanion of the triple-decker.

Reduction of the CoNi compound in CH_3CN was not chemically reversible. A follow-up reaction of the anion, presumably with acetonitrile, was observed, making this the only monoanion of the four compounds reported here that was unstable in this solvent. The data supporting this come from cyclic voltammetry, polarography, and controlled-potential coulometry. At faster CV scan rates (above 1 V/s), the reduction was reversible, with $E°$ = −1.66 V and Δe_p ca. 60 mV. But at slower scan rates, the anodic peak due to reoxidation of $CoNi^-$ disappeared and a new anodic peak at −1.48 V grew in. This must be due to a new product, formed by reaction of the triple-decker anion with solvent. The new oxidation wave was irreversible. At *slower* scan rates the cathodic current function ($i_{p_c}/v^{1/2}$) increased until it was almost the value appropriate for a two-electron reduction. This was confirmed by the dc polarographic measurements, also a longer time scale experiment, in which the I_d value (5.25) was close to double that of the one-electron $(C_5H_5)_2Co^+$ standard. Controlled-potential coulometry at a Pt basket at −1.85 V in CH_3CN gave an n value of 2.3 electrons (the solution was brown), and two resulting waves, both irreversible, one being the oxidation at −1.48 V, the other being a reduction at −2.59 V. Thus, the reduction of **15a** in CH_3CN is seen to be an ECE-type process, in which a chemical reaction following the initial electron transfer gives rise to a species undergoing a further one-electron reduction. Since the potentials of the electrolysis products do not match those[39] of the quadruple-decker compound **20b**, it is likely that the products are monometallic, in which one $(C_5H_5)M$ fragment has been removed from the triple-decker. This kind of tendency to lose one metal fragment has been observed previously with charged triple-deckers, namely for $(C_5H_5)_3Ni_2^+$[4] and $[(C_5H_5)Co(C_8H_8)Co(C_5H_5)]^{2+}$, in coordinating solvents.[40]

Summarizing the situation for **15a**, we see that by judicious choice of solvent (CH_2Cl_2 for oxidation, THF for reduction), a four-membered electron-transfer series to stable species is encountered (below) encompassing 30–33-electron triple-decker compounds. The anion and dication decompose rapidly in acetonitrile:

$$CoNi^{2+} \rightleftharpoons CoNi^+ \rightleftharpoons CoNi^0 \rightleftharpoons CoNi^-$$

$(C_5H_5)Ni(C_2B_2C)Ni(C_5H_5)$ (14a). This 33-electron compound gave rise to one reversible reduction ($E°$ = −1.31 V) and two oxidations, only the first of which was reversible ($E°$ = 0.13 V). The dc polarogram of this compound (Figure 9), in which one reduction and one oxidation are observable, is typical of the polarographic data on the triple-deckers (Table XIV). When probed by cyclic voltammetry, the second oxidation was irreversible in acetonitrile (anodic peak potential of +1.25 V) or dichloromethane (+1.49 V). Bulk oxidation of this compound at Pt in either solvent at +0.2 V released one electron (n = 0.9e$^-$), and the solution changed from deep green to pea-green. CV scans showed that the monocation was the only electrolysis product, and the neutral compound could be quantitatively regenerated by rereduction of the solution at −0.16 V. Bulk reduction at −1.60 V in CH_3CN, at a mercury pool, gave solutions of the monoanion that spontaneously reverted back to the neutral compound, apparently through reaction with adventitious oxygen. The monoanion of **14a** was better prepared by reduction with alkali metal (vide ante).

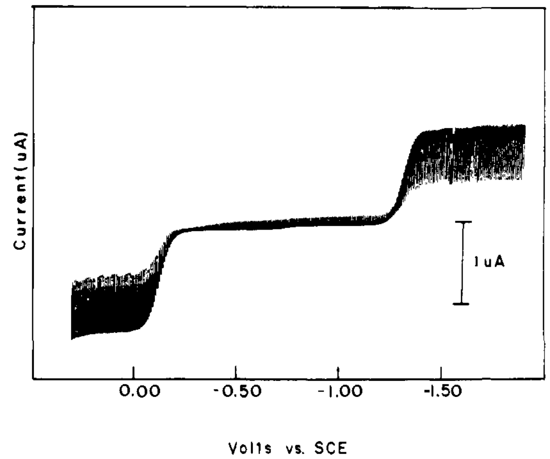

Figure 9. A dc polarogram of 0.3 mM of NiNi triple-decker (**14a**) in CH_3CN/Bu_4NPF_6 at the DME; v = 2 mV/s; t = 2 s.

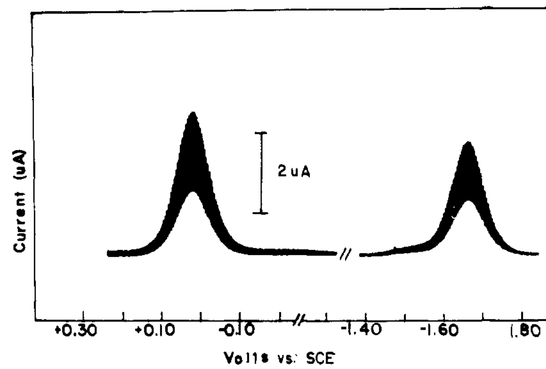

Figure 10. Phase-selective ac polarogram of the in-phase components of the CoNi triple-decker complex in CH_3CN/Bu_4NPF_6 at a DME; v = 2 mV/s; t = 2 s; frequency = 100 Hz.

Thus the dinickel compound was seen to have an electron-transfer series involving just three stable species, from the 32-electron cation to the 34-electron anion.

$$\text{“}NiNi^{2+}\text{”} \leftarrow NiNi^+ \rightleftharpoons NiNi^0 \rightleftharpoons NiNi^-$$

The 31-electron dication is very unstable and, whereas its existence is implied in the one-electron nature of the oxidation of $NiNi^+$, we have no direct evidence of it. One of the most interesting features of this series is that we find no evidence of any reductions beyond the 34-electron case. This was predicted by Hoffmann et al.[6] to be the maximum number of valence electrons that could be accommodated by triple-decker sandwiches. Reduction of the neutral dinickel compound to the 34-electron $NiNi^-$ occurs at a relatively mild potential (−1.3 V), and another 1.5 V of negative potential was available in our experiments before electrolyte breakdown (−2.8 V). Since no further reductions were found, these results are clearly consistent with the LUMO orbital in a 34-electron triple-decker being rather high in energy.

Electron-Transfer Rate Measurements. CV studies of these compounds did not indicate any slow electron-transfer steps. That is, all redox processes seemed to be electrochemically reversible. We obtained quantitative measurements of electron-transfer rates

(39) W. Geiger, unpublished results.
(40) Moraczewski, J.; Geiger, W. E. *J. Am. Chem. Soc.* **1978**, *100*, 7429.

Table XV. Standard Heterogeneous Electron-Transfer Rates, k_s, for Triple-Decker Compounds[a]

triple-decker	couples	$E°$	k_s[b]
FeCo (**17a**)	+/0	−0.06	0.76
	0/−	−1.77	1.5
CoCo (16a)	+/0	−0.57	0.44
	0/−	−1.53	0.74
NiCo (**15a**)	+/0	+0.03	2.3
	0/−	−1.66	2.2
NiNi (**14a**)	+/0	−0.13	2.3
	0/−	−1.31	1.9

[a] Measured by phase-selective ac polarography at dropping mercury electrode; 0.1 M Bu_4NPF_6 in CH_3CN. [b] Standard (uncorrected) rate constant in cm/s.

with phase-selective ac polarography. Ac polarograms were as expected[41] for essentially reversible one-electron waves (Figure 10): peak widths at half-height were 90–100 mV; peak currents were proportional to square root of ac frequency; the cotangent of the angle, ϕ, between applied potential and detected current was proportional to the square root of ac frequency. Slopes of the latter curves (Figure 10) were used to calculate the standard heterogeneous electron-transfer rate, k_s, by the method of Smith.[41] Results are shown in Table XV. All of the rate constants fall into the range associated with reversible electron-transfer reactions, implying that there is little structural change occurring in the electron-transfer reactions of these compounds and that the electron-transfer rates are limited by solvent reorganization in the charge-transfer step.

Discussion

For the construction of the triple-decker complexes **14–17** with 33–30 valence electrons, several routes have been studied, which involve either a stacking of a sandwich (**13** or **18**, respectively, the latter as a neutral or anionic complex) or an interaction of the free ligand **6** with a mono- or dinuclear carbonyl compound. The Lewis acid sandwiches **13** and **18** possess good acceptor qualities and therefore undergo stacking reactions with the isolobal[6] cyclopentadienylmetal moieties $(C_5H_5)M$ (M = Fe, Co, Ni) to give **14–17** in moderate to excellent yields. In particular the stacking of **13** to **14** and **15**, respectively, is accompanied by hardly any side reactions. Because of the high reactivity of the free ligand **6** its reaction with carbonylmetal complexes often leads to byproducts, since even at room temperature **6** is attacked by the released carbon monoxide.[16] Insertion of CO into the boron–carbon bonds of **6** and rearrangement of the formed intermediates yield two isomeric six-membered C_3B_2O heterocycles. The 1,3-dibora-2-oxacyclohexene isomer in which a C_3 unit is bridged by the B–O–B group forms with $Ni(CO)_4$ a bis(1,3-dibora-2-oxacyclohexenyl)nickel complex.[16]

The only example where apparently no CO insertion into B–C bonds occurs is the reaction of **6** with $[(C_5H_5)Ni(CO)]_2$, which results in high yields of the triple-decker sandwich **14**. We assume that either the coordinatively unsaturated monomeric species $[(C_5H_5)Ni(CO)]$ or the dimer with one terminal and one bridging CO group are the reactive intermediates. It is likely that once **6** is complexed to the nickel atom in an η^2 or η^4 fashion, the carbon monoxide cannot insert anymore into the B–C bonds. Elimination of hydrogen and CO from the initially formed complex then leads to the η^5-bonded diborolenyl ring.

Depending on the molar ratio of **6** and $[(C_5H_5)Ni(CO)]_2$, one obtains either the sandwich **13** or the triple-decker sandwich **14** as the main product[13] (Scheme VI). Since a cleavage of **14** by **6** to yield **13** is not observed under conditions used for the synthesis of **13**, it is evident that the formation of **14** proceeds via stacking of the sandwich **13** and not via insertion of **6** into the Ni–Ni bond of an intact $[(C_5H_5)Ni(CO)]_2$ molecule.

Unfortunately the CO insertion hampers the synthesis of the cobalt-containing triple-decker sandwiches **16** and **17** starting from

Scheme VI

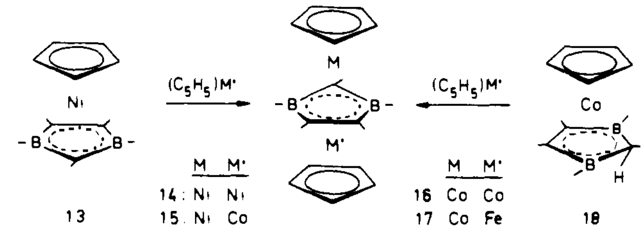

Scheme VII

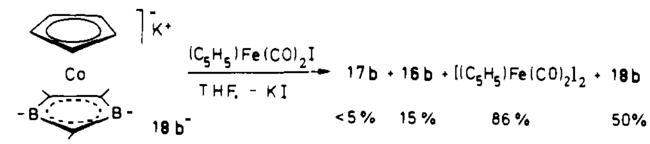

the ligands **6a,b** and the corresponding carbonylmetal complexes. During the preparation of the paramagnetic **16** we had found traces of the red sandwich complex **18**, which was assumed to be the intermediate en route to **16**. This hypothesis could subsequently be confirmed by an independent synthesis[17] of **18** from **6** and cyclopentadienylbis(ethene)cobalt.[42]

The use of $(C_5H_5)Co(C_2H_4)_2$ for $(C_5H_5)Co(CO)_2$ as a supplier of the $(C_5H_5)Co$ d^8 fragment improved the access to the triple-deckers **16** and **17** (Scheme VII). Furthermore it has opened the chemistry of the novel sandwich complex **18** having a pentacoordinated carbon atom and an axial hydrogen atom. The constitution of **18a** was confirmed by an X-ray structure analysis; the exact location of the axial hydrogen, however, is at present uncertain. Presumably this hydrogen is bonded in a three-center two-electron fashion Co···C···H via an orbital with strong p character, since $^1J_{^{13}C,H}$ is only about 70 Hz.[17] Thermal reactions cause the replacement of the axial hydrogen in **18** with the isolobal $(C_5H_5)M$ fragments (M = Fe, Co, Ni), which supply for the bonding besides three orbitals one, two, and three electrons, respectively. One might expect that ionic species would lead to triple-decker arrangements under mild conditions. However, the anionic sandwich **18b**$^-$ and $(C_5H_5)Fe(CO)_2I$ yield only minor amounts of the FeCo triple-decker **17b** and some **16b** besides **18b** and $[(C_5H_5)Fe(CO)_2]_2$ (Scheme VII). This indicates a redox reaction leading on one side to the neutral sandwich **18b** via the radical **18b**·, which picks up a hydrogen atom from the solvent, and on the other side to the cyclopentadienyliron dicarbonyl dimer. An analogous sequence is observed in the reaction of **18**$^-$ with R_2BX and R_3SiX, respectively, yielding the neutral sandwich **18**.[19] Although the boryl group R_2B supplies two orbitals for bonding, no borylated sandwich is formed. With the RBe group, however, a dinuclear compound with a C_3B_2Co cluster is expected, since the RBe entity contributes one electron and three orbitals as $(C_5H_5)Fe$ does.

In summarizing the synthetic approaches to triple-deckers, it is of interest that the complexes with 32 and 33 valence electrons (**15**, **14**) are most easily obtained, whereas **16** and **17**, the cobaltocene and ferrocene analogues, are more difficult to prepare. The opposite would be expected on the basis of electronic considerations.

Let us turn now to the chemical relationship between the sandwich series ferrocene and cobaltocene as well as nickelocene and their electronic counterparts in the triple-decker series **17**, **16**, and **15** with 30, 31, and 32 valence electrons, respectively. These dinuclear species are formally obtained by inserting the 12 VE stack 1,3-diborolenylcobalt $[(C_2B_2C)Co]$ into the C_5H_5–M bond of the metallocenes. The introduction of the Lewis acid 1,3-diborolenyl ligand into metallocenes lowers the electron density in the C_5H_5 rings. As a result the C_5H_5 rings in $(C_5H_5)Fe(C_2B_2C)Co(C_5H_5)$ lose their susceptibility to electrophilic substitution.

(41) Smith, D. E. In "Electroanalytical Chemistry"; Bard, A., Ed; Marcel Dekker: New York, 1966; Vol. 1, p 1.

(42) Jonas, K.; Krüger, C. *Angew. Chem.* **1980**, *92*, 513: *Angew. Chem., Int. Ed. Engl.* **1980**, *19*, 520.

They are not borylated by BBr_3, whereas the unique ferrocene and BBr_3 react in refluxing carbon disulfide to yield $(C_5H_5)Fe(C_5H_4BBr_2)$ and $Fe(C_5H_4BBr_2)_2$.[43] One example of the close chemical relationship between 20 VE nickelocene and the 32 VE NiCo triple-decker **15** is the insertion of the $(CO)_3Fe$ fragment into the $(C_5H_5)Ni$ bond of both compounds. The initially obtained trinuclear complex **22** forms on heating the novel tetranuclear compound **23**, which is the electronic analogue of $[(C_5H_5)Ni(CO)]_2$, into which two $(C_2B_2C)Co$ fragments are inserted.

As already pointed out in the introduction, nickelocene and HBF_4 result in the red 34 VE triple-decker cation $(C_5H_5)_3Ni_2^+$.[4] A further analogy seems to occur in the reaction of **15** with HBF_4 leading to a dark red product, for which a pentuple-decker structure is likely.[44]

Finally, the behavior of the NiCo triple-decker **15** parallels that of nickelocene upon chemical reduction. The anion **15**$^-$ cleaves off $C_5H_5^-$ as nickelocene does; however, the formed fragment **19** stabilizes itself by forming the quadruple-decker sandwich **20** in high yields.

For an understanding of the chemical reactivity the structures of the triple-decker sandwich complexes **14–17** are of considerable interest. The first examples[14,15] of this triple-decker family exclusively contained the tetraethylmethyldiborolenyl ligand **6a** in the bridging position, and the constitution of the diamagnetic species (**17a**, **14a**$^-$) was derived from spectroscopic data (MS, ^{11}B and ^1H NMR). There was no reason to assume a different structure for the paramagnetic complexes **14a**, **15a**, and **16a**. In order to confirm the proposed triple-decker structures, X-ray investigations were initiated; however, all attempts on crystals of **14a–17a** failed, because of the poor quality of the material. This is caused by the four ethyl groups in the central ligand **6a**. We finally succeeded in obtaining suitable crystals of **14**, **15**, and **17** with the new diborolene ligand **6b**, which was synthesized from 3,4-diethyl-2,5-diiodo-1,2,5-thiadiborolene[45] and $(C_5H_5)_2Ti(Cl)CH_2Al(CH_3)_2$[46] in 35% yield. However, despite numerous attempts we have not been able to grow good crystals of the CoCo triple-decker **16b**. For this missing member of the family we estimate a metal–metal distance Co···Co = 3.27 Å on the basis of 3.20 in the FeCo, 3.33 in the NiCo, and 3.41 Å in the NiNi compound. A value of 3.20 Å for FeCo was expected considering the metal–metal distances in the related 30 VE triple-decker sandwiches bis(cyclopentadienylcobalt)-μ-dicarbatriboranes[5,47,48] **2** and **3** (3.14 Å) and a derivative of bis(cyclopentadienyliron)-μ-boracyclopentadiene[49] (3.27 Å).

The nature of the bonding in the bis(cyclopentadienylmetal)-μ-diborolenyl complexes has already been discussed. Throughout this paper these compounds are regarded as sandwich complexes, in which two metals are sandwiched between two C_5H_5 rings and the bridging ligand. For **17** the number of 30 valence electrons is given by a π^6, d^6, π^4, d^8, and π^6 configuration.

An alternative view of these dinuclear compounds is that of a C_3B_2MM' seven-vertex cluster, having 16 framework electrons, which are supplied for **17'** by CpCo (2), CpFe (1), two RB (4) and three RC (9). This number is required by the "$2n + 2$" rule[50] for closo clusters. For a compound with adjacent boron atoms in **17**[51] we expect a rearrangement of the cluster 1,7,2,3,4-$FeCoC_3B_2$ to the 1,7,2,3,5-$FeCoC_3B_2$ isomer (**17'**) on the surface of a seven-atom polyhedron, as has been demonstrated for **2**, which at higher temperatures rearranges to **3**.[52]

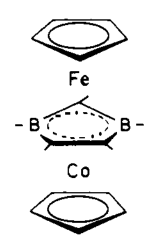

17

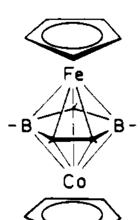

17'

Since the paramagnetic triple-decker **16**, **15**, and **14** as well as the diamagnetic **14**$^-$ contain one–four electrons more than required, the rules for cagelike compounds[50] predict an opening of the cage, as it is found in boranes and carboranes. In our case no opening is observed but an expanding of the cluster, as a result of filling slightly antibonding orbitals.[8a]

Several important observations are possible from the redox data. First, only one-electron charges were observed. This clearly implies that there is a high degree of charge delocalization in the ions derived from these triple-deckers. This lends further evidence to the growing body of information that suggests that the triple-deckers do not have metals that are isolated electronically from each other.

Second, at least three different "oxidation states" having reasonable stability were observed for each triple-decker. Overall, stable compounds possessing from 29 to 34 valence electrons were encountered. It is evident, therefore, that great variations are possible in the electronic structures of extended-chain π complexes without disruption of the chain. Third, no complexes having even a transient existence with more than 34 electrons were found. As stated earlier, this is consistent with the bonding model of tri-

Table XVI. Summary of Reduction Potentials of Triple-Decker Compounds in CH_3CN[a]

compound	$E°$ (2+/1+)	$E°$ (1+/0)	$E°$ (0/1−)	$E°$ (1−/2−)
$CpFe(C_2B_2C)CoCp$ (17a)		−0.06[b,c]	−1.77[b,c]	
$CpCo(C_2B_2C)CoCp$ (16a)	+1.74[c,d]	−0.57[b,c]	−1.53[b,c]	−2.56[c,d]
$CpCo(C_2B_2C)NiCp$ (15a)	+1.00[c−e]	+0.03[b,c]	−1.66[b,c]	
$CpNi(C_2B_2C)NiCp$ (14a)	+1.26[c,d]	−0.13[b,c]	−1.31[b]	

[a] Potentials reported vs. aqueous saturated calomel electrode. [b] Measured by dc polarography. [c] Measured by cyclic voltammetry. [d] Peak potential given. [e] Reversible in CH_2Cl_2, $E°$ = +1.08 V.

Table XVII. Observed Triple-Decker Redox States, Categorized by the Number of Valence Electrons

29e⁻	30e⁻	31e⁻	32e⁻	33e⁻	34e⁻
$FeCo^+$	FeCo	$FeCo^-$			
$CoCo^{2+}$ [a]	$CoCo^+$	CoCo	$CoCo^-$	$CoCo^{2-}$	
	$CoNi^{2+}$	$CoNi^+$	CoNi	$CoNi^-$	
		$NiNi^{2+}$	$NiNi^+$	NiNi	$NiNi^-$

[a] The CoCo dication has a very transient existence. Consult text for details.

Table XVIII. Relative Energies of the Observed Redox Products in the Series FeCo (17b), CoCo (16b), NiCo (15b), and NiNi (14b) according to the Semiempirical INDO Calculations[a]

compd	oxidation state +2	+1	0	−1	−2
FeCo		6.89	0.00	−3.14	
CoCo	19.81	8.20	0.00	−3.88	−1.81
NiCo	20.84	8.20	0.00	−3.12	
NiNi	20.23	7.65	0.00	−1.49	

[a] The total energies of the neutral triple-decker compounds have been used as internal standard; all values in electron volts. The geometries of the ions correspond to the geometry at the neutral complex.

(43) Renk, Th.; Ruf, W.; Siebert, W. *J. Organomet. Chem.* **1976**, *120*, 1.
(44) T. Grell, W. Siebert, unpublished results, 1982.
(45) Siebert, W.; Full, R.; Renk, Th.; Ospici, A. *Z. Anorg. Allg. Chem.* **1975**, *418*, 273.
(46) Tebbe, N. F.; Parshall, G. W.; Reddy, G. S. *J. Am. Chem. Soc.* **1978**, *100*, 3611.
(47) Robinson, W. T.; Grimes, R. N. *Inorg. Chem.* **1975**, *14*, 3056.
(48) Pipal, J. R.; Grimes, R. N. *Inorg. Chem.* **1978**, *17*, 10.
(49) Herberich, G. E., III. International Meeting on Boron Chemistry, Ettal (FRG), 1976.
(50) Wade, K. *J. Chem. Soc., Chem. Commun.* **1971**, 792; *Adv. Inorg. Chem. Radiochem.* **1976**, *18*, 1.
(51) Siebert, W. *Nachr. Chem., Tech. Lab.* **1977**, *25*, 597.
(52) Grimes, R. N. *Pure Appl. Chem.* **1974**, *39*, 455. Miller, V. R.; Grimes, R. N. *J. Am. Chem. Soc.* **1975**, *97*, 4213; *Coord. Chem. Rev.* **1979**, *28*, 47.

Table XIX. Calculated Net Charges of the Various Molecular Fragments (3d Center, Ligands) for the Observed Redox Products of FeCo (**17b**) and NiCo (**15b**) according to the INDO Model

compd	fragment[a]	oxidation state +2	+1	0	−1
FeCo	Cp_{Co}		0.042	−0.190	−0.561
	Co		0.805	0.782	0.791
	C_3B_2		−0.716	−1.025	−1.392
	Fe		0.727	0.556	0.543
	Cp_{Fe}		0.142	−0.123	−0.381
NiCo	Cp_{Ni}	0.290	−0.037	−0.450	−0.776
	Ni	0.926	0.954	1.034	0.922
	C_3B_2	−0.454	−0.737	−0.993	−1.301
	Co	0.791	0.790	0.786	0.732
	Cp_{Co}	0.447	0.030	−0.377	−0.577

[a] The indices at the Cp fragments (Co, Fe, Ni, Co) are used for the classification of the two topologically different Cp units.

ple-deckers in which the LUMO of 34-electron compounds is highly antibonding.

Redox potentials themselves are very limited parameters with which to probe electronic structure. In a related group of molecules involving an extensive electron-transfer series, it is sometimes informative to compare differences in potential between successive redox steps. Using the $E°$ potential summarized in Table XVI, we found no clear trends in spacings of $E°$ potentials, except that $\Delta E°$ values for interconnecting $29 \rightleftharpoons 30 \rightleftharpoons 31$ electron species are much larger than those interconnecting $30 \rightleftharpoons 31 \rightleftharpoons 32$ electron species. In Table XVII, we have collected the redox couples according to the number of valence electrons in the compound to facilitate comparisons.

The results of semiempirical INDO calculations are in line with the experimental findings in the electrochemical measurements. In Table XVIII we have summarized the relative energies for all observed redox products in the series of the FeCo, CoCo, NiCo, and NiNi derivatives. The total energy of the neutral triple-decker complexes has been selected as internal reference. It is seen that the dicationic species in CoCo, NiCo, and NiNi are highly unstable with respect to their monocationic counterparts and with respect to their neutral parents. In the case of the monoanionic systems the stabilities of $FeCo^-$, $CoCo^-$, and $NiCo^-$ on one side differ dramatically from the stability of the $NiNi^-$ ion on the other side. The dianionic $CoCo^{2-}$ compound is highly unstable with respect to the formation of the monoanion, a theoretical result that exactly parallels the electrochemical data.

For the NiCo anion obtained from NiCo and potassium in ether (vide ante) it has been demonstrated that this species is unstable, and the formation of a quadruple-decker complex in high yield occurs. In acetonitrile an unknown decomposition of the triple-decker has been detected. This behavior of the $NiCo^-$ anion is expected on the basis of the Wiberg bond indices for $NiCo^-$ that are displayed in Figure 2. The bond indices between Ni and the two ligands (cyclopentadienyl, diborolenyl fragment) are small in comparison to the Co ligand indices and small in comparison to the other values summarized in Figure 2. It is seen that the covalent interaction between the Ni center and the two ligands is comparable. Two fragmentation schemes of the complex therefore should be possible: the cleavage into the cyclopentadienyl anion and a dinuclear neutral metal fragment or the fragmentation into the $(C_5H_5)Ni$ fragment and a heterocyclic sandwich anion $[(C_5H_5)Co(C_2B_2C)]^-$. On the basis of the calculated Wiberg indices both types of decomposition should be facilitated in a polar medium solvating the ionic fragments.

The electrochemical measurements have furthermore indicated that the charges are largely delocalized in the cationic and anionic species. This is supported by the INDO results of Table XIX where the fragment net charges of the FeCo complex **17b** and the NiCo derivative **15b** are summarized for all observed redox products. The modification of the net charges at the 3d centers is small in comparison to the variation at the ligands. The strongest charge redistributions are always encountered in the central diborolenyl ring, indicating the bivalent character of the C_3B_2 fragment in triple-decker complexes as a potential electron donor and acceptor.

Experimental Section

Methods. All reactions and manipulations were carried out under an atmosphere of purified and dried nitrogen using Schlenk-type glassware. The solvents were dried by standard methods, distilled from sodium/benzophenone ketyl, and kept under nitrogen. Column chromatography was carried out under nitrogen atmosphere on silica gel Woelm 100–200, which was heated for 4–5 h at 150–160 °C in vacuo. Melting points were determined by using a Reichert melting point apparatus (capillary method) and are uncorrected. Microanalyses were performed by the microanalysis laboratories of the Fachbereich Chemie, Universität Marburg, and of the Organisch-Chemisches Institut, Universität Heidelberg.

Spectral Measurements. The ^1H NMR spectra (δ, Me_4Si) were recorded on a Varian EM-360, a Varian XL-100, or a JEOL 300 spectrometer, the ^{11}B NMR spectra (δ, $Et_2O{\cdot}BF_3$) on a Varian XL-100 spectrometer, and the ^{13}C NMR spectra were measured on a Varian XL-100 or a Varian CFT-20 spectrometer. The mass spectra were obtained with a Varian MAT CH7, a MAT 711, or a VEGE 700 spectrometer.

ESR data were recorded with an x-band spectrometer, Varian V4500-10A with a 9-in. magnet. Most spectra were measured at liquid nitrogen temperature (77 K), and diphenylpicrylhydrazyl (DPPH) was used as a g value standard. Samples of cation radicals were taken after bulk electrolytic oxidation of the neutral compounds, and anion radical spectra were obtained by alkali metal reduction of the neutral precursors. Metal reductions were done under high vacuum with sodium/potassium alloy in one chamber of a special cell with a few milligrams of the compound to be reduced in another chamber. Solvent (THF) was distilled into the chamber containing the compound, and the resulting solution was mixed with the alloy at a reduced temperature (usually about 200 K). After evidence of reaction (color change) the solution was tipped into a quartz side arm on the cell and frozen in liquid nitrogen for ESR analysis.

The Mössbauer spectra of polycrystalline samples of **17b** (FeCo) and $\mathbf{17b}^+BF_4^-$ were obtained with a conventional velocity-scanning spectrometer, in conjunction with a multichannel analyzer in the multiscalar mode. The room-temperature source consisted of about 40 mCi of ^{57}Co diffused into metallic Rh. The spectra were measured in the velocity range about ±4.8 $mm{\cdot}s^{-1}$ at several temperatures between 10 and 295 K by employing the technique of blowing cold helium or nitrogen gas over the sample. The temperature accuracy was about 2 K while temperature stability was somewhat better. The velocity transducer was calibrated with the conventional method of employing the Mössbauer spectra of metallic iron. We found the linearity for the velocity range better than 1%. The spectra at 4.2 K were obtained without and with a superconducting solenoid whereby source and probe were held at liquid helium temperature.

A Princeton Applied Research FM-1 vibrating sample magnetometer, coupled with a Janis liquid helium Dewar, was used for the determination of the magnetic susceptibility of $\mathbf{17b}^+BF_4^-$. Temperatures were adjusted and measured by using a Gatts diode. Empty-holder diamagnetic corrections were applied throughout the whole temperature range. The temperature accuracy was better than 2 K.

Electrochemical Procedures. Tetrahydrofuran (Aldrich, anhydrous) was stirred over and then flash distilled from lithium aluminum hydride into a flask containing sodium and benzophenone and was stored in vacuo over the resulting ketyl. It was distilled from this storage flask into a receiver vessel in a bulb-to-bulb vacuum distillation just prior to each electrochemical experiment. Methylene chloride (Aldrich) was distilled from calcium hydride and acetonitrile (Aldrich spectrograde) was used as received. The supporting electrolyte for all solvents was 0.1 M tetra-n-butylammonium hexafluorophosphate (Bu_4NPF_6). The electrolyte was prepared by metathesis of Bu_4NI (Eastman) and ammonium hexafluorophosphate (Ozark-Mahoning) in acetone, followed by filtration of NH_4I and precipitation of the desired salt by addition of water. It was recrystallized several times from 95% ethanol and vacuum-dried.

Since the compounds investigated are all air-stable materials, most of the electrochemical measurements were accomplished by using benchtop techniques and a nitrogen purge to exclude oxygen. Bulk coulometry was, however, performed inside a Vacuum Atmospheres drybox. Voltammetric experiments were performed by using a Princeton Applied Research Model 173 potentiostat, a Model 179 digital coulometer, and a Model 175 function generator. Slow sweep-rate data were recorded on a Hewlett-Packard Model 7001A X-Y recorder and faster experiments were recorded on a Tektronix Model 564B storage oscilloscope. Potentials, all referred to the aqueous saturated calomel electrode (SCE), were checked by using a Keithly digital voltmeter.

Experiments were performed at either mercury or platinum. Mercury was obtained as triply distilled from Bethlehem Apparatus Co. The platinum electrode was a small button sealed through the end of a glass tube. It was pretreated by refluxing in concentrated nitric acid, washing with distilled water, and then soaking in a saturated solution of ferrous ammonium sulfate in 1 M H_2SO_4. It was inserted into solution after washing with water and wiping dry.

Bulk coulometry was accomplished by using a two-compartment cell in which the cathodic and anodic compartments were separated by a 20-mm fine frit. The working electrode was either a mercury pool or a platinum gauze cylinder. A platinum basket was placed in the auxiliary electrode compartment, which was placed either parallel to the working electrode (in case of mercury pool) or inside of it (platinum cylinder).

Preparation of the 1,3-Diborolenes 6a and 6b. 2-Methyl-1,3,4,5-tetraethyl-Δ^4-1,3-diborolene (**6a**) was prepared as described by Bingen.[53] Reaction of $B(C_2H_5)_3$ and NaH yielded $[(C_2H_5)_3BH]^-Na^+$, which on treatment with $C_2H_5C{\equiv}CH$ afforded $[(C_2H_5)_3BC{\equiv}CC_2H_5]^-Na^+$. The latter resulted with $(C_2H_5)_2BCl$ the formation of *cis*-hexaethyldiborylethene, which on pyrolysis at 160 °C for 5 h yielded a yellow-orange reaction mixture. Distillation at 90–93 °C (4–6 torr) afforded air-sensitive **6a** (35–45%).

To a suspension of 12.0 g (30.8 mmol) of 4,5-diethyl-1,3-diiodo-Δ^4-1,2,5-thiadiborolene[45] in 60 mL of cooled benzene was slowly added 9.0 g (31.6 mmol) of $(C_5H_5)_2Ti(CH_2)ClAl(CH_3)_2$[46] in 50 mL of benzene. After stirring for 2 h, the solution was allowed to warm to room temperature, and two-thirds of the solvent was removed at 20 °C (50 torr). The remaining volatile products were distilled at 20 °C (0.01 torr) into a cooled trap. After the solvent was removed at 20 °C (30 torr), 4,5-diethyl-1,3-dimethyl-Δ^4-1,3-diborolene (**6b**) was distilled at 73–75 °C (30 torr), yielding 1.6 g (35%) of colorless, air-sensitive liquid: ^{1}H NMR (100 MHz, C_6D_6) δ 2.32 (q, 4), 1.35 (s, 2), 0.98 (t, 6), 0.90 (s, 6); ^{11}B NMR δ 7.17. Due to its high reactivity no satisfactory C,H analysis of **6b** could be obtained.

Preparation of (η^5-Cyclopentadienyl)(η^5-4,5-diethyl-1,3-dimethyl-1,3-diborolenyl)nickel (13b). To a solution of 0.90 g (2.90 mmol) of $[(C_5H_5)Ni(CO)]_2$ in 20 mL of mesitylene, 0.80 g (5.4 mmol) of **6b** were added. Upon heating (150–160 °C for 2 h) the reaction mixture turned deep red. The solvent was removed at room temperature in vacuo (0.1 torr). The residue was dissolved in 40 mL of hexane and filtered through a GII frit. After removing the hexane, 1.1 g (75%) of the red sandwich **6b** was isolated by vacuum distillation, bp 56–58 °C (0.01 torr), mp 39–41 °C. Small amounts of the green triple-decker sandwich **14b** remained in the distillation flask. Mass spectrum, *m/z* (relative intensity) 270 (M^+, 100), 255 ($M^+ - CH_3$, 10), 241 ($M^+ - C_2H_5$, 48.9), 204 (65.1); ^{1}H NMR (C_6D_6) δ 0.94 (s, 6), 1.08 (t, 6), 2.1 (m, 4), 4.30 (s, 1), 4.72 (s, 5); ^{11}B NMR (C_6D_6) δ 36.4; ^{13}C NMR (C_6D_6) δ −1.2 (br, BCH_3), 15.5 (s, CH$_3$), 23.7 (s, CH$_2$), 84 (br, CH), 91.2 (s, Cp), 129 (br, C=C). Assignment of the signals was possible in a gated decoupled spectrum. Anal. Calcd for $C_{14}H_{22}B_2Ni$ (270.6): C, 62.13; H, 8.19. Found: C, 62.25; H, 8.40. **13a** was obtained analogous to **13b** from **6a** and $[(C_5H_5)Ni(CO)]_2$; yield 64%, mp 51 °C.[13]

Preparation of (μ-2-Methyl-1,3,4,5-tetraethyl-1,3-diborolenyl)bis((η^5-cyclopentadienyl)nickel) (14a). **13a** [0.30 g (0.96 mmol)] and $[(C_5H_5)Ni(CO)]_2$ [0.16 g (0.53 mmol)] in 5 mL of mesitylene were heated for 3 h at 150 °C, whereby the initially deep red solution turned to deep green.[14] After removing the solvent in vacuo, the triple-decker was sublimed from the reaction flask at 120–130 °C (0.01 torr), yielding 0.40 g (96%). **14a** was also obtained by refluxing a solution of 0.63 g (3.32 mmol) of **6a** and 1.01 g (3.33 mmol) of $[(C_5H_5)Ni(CO)]_2$ in 10 mL of toluene for 10 h. After the solvent was removed in vacuo, a deep green, sticky residue remained, which was chromatographed with a silica gel column (25 cm, *n*-hexane). First red **13a** appeared (0.06 g, 6%) which was followed by green **14a** (0.78 g, 54%). **14a** is air-stable and dissolves readily in organic solvents. It sublimes in a sealed capillary above 110 °C and melts above 200 °C. Mass spectrum, *m/z* 435 (M^+, 100), 123 ($CpNi^+$, 7); high-resolution MS, *m/z* 435.1475, calcd for $^{12}C_{22}H_{33}{}^{11}B_2{}^{58}Ni_2$ 435.1476 amu. Anal. Calcd for $C_{22}H_{33}B_2Ni_2$ (436.5): C, 60.53; H, 7.62; Ni, 26.90. Found: C, 60.52; H, 7.53; Ni, 26.93.

(μ-4,5-Diethyl-1,3-dimethyl-1,3-diborolenyl)bis((η^5-cyclopentadienyl)nickel) (14b) was obtained as described for **14a**: 0.90 g (2.90 mmol) of $[(C_5H_5)Ni(CO)]_2$ and 0.40 g (2.70 mmol) of **6b** were refluxed (3 h) in 10 mL of mesitylene. Sublimation at 110–120 °C (0.01 torr) yielded 0.90 g (85%) green **14b**: mp 185 °C; mass spectrum, *m/z* 394 (M^+, 100). Anal. Calcd for $C_{19}H_{27}B_2Ni_2$ (394.5): C, 57.84; H, 6.89. Found: C, 57.55; H, 6.78.

Preparation of (η^5-Cyclopentadienyl)nickel(μ-2-methyl-1,3,4,5-tetraethyl-1,3-diborolenyl)(η^5-cyclopentadienyl)cobalt (15a). A solution of 1.20 g (3.84 mmol) of **13a** and 1.00 g (5.55 mmol) of $(C_5H_5)Co(CO)_2$ in 10 mL of mesitylene was refluxed for 4 h, which caused a change from deep red to blue green. After the solvent was removed in vacuo, **15a** was sublimed at 120–130 °C (0.01 torr); yield 1.48 g (88%); mp: above 120 °C sublimation, >200 °C melting; mass spectrum, *m/z* 436 (M^+, 100), 189 (Cp_2Co^+, 43), 124 ($CpCo^+$, 3), 123 ($CpNi^+$, 3); high-resolution MS, *m/Z* 436.1456, calcd for $^{12}C_{22}H_{33}{}^{11}B_2{}^{58}Ni^{59}Co$ 436.1453 amu. Anal. Calcd for $C_{22}H_{33}B_2CoNi$: C, 60.50; H, 7.62; Co, 13.49; Ni, 13.44. Found: C, 61.01; H, 7.44; Co, 13.36; Ni, 11.86.

(η^5-Cyclopentadienyl)nickel(μ-4,5-diethyl-1,3-dimethyl-1,3-diborolenyl)(η^5-cyclopentadienyl)cobalt (15b) was obtained analogous to **15a**: 0.50 g (1.84 mmol) of **13b** and 0.80 g (4.4 mmol) of $(C_5H_5)Co(CO)_2$ yielded 0.60 g (78%) of blue-green **15b**, which was sublimed at 110–120 °C (0.01 torr). A green product remained as a residue and was identified by mass spectroscopy as the quadruple-decker sandwich **20b**: mass spectrum, *m/z* 394 (M^+, 100); mp, 190 °C. Anal. Calcd for $C_{11}H_{27}B_2CoNi$ (394.7): C, 57.82; H, 6.90. Found: C, 57.99; H, 6.96.

Preparation of (μ-2-Methyl-1,3,4,5-tetraethyl-1,3-diborolenyl)bis((η^5-cyclopentadienyl)cobalt) (16a). A solution of 0.75 g (3.95 mmol) of **6a** and 1.72 g (9.60 mmol) of $(C_5H_5)Co(CO)_2$ in 5 mL of mesitylene was refluxed for 5 h, which caused a change from red to green-brown. After the addition of 50 mL of *n*-hexane the solution was filtered through a glass frit and chromatographed on a silica gel column. **16a** appeared as an olive-green product, which was sublimed at 120–130 °C (0.01 torr), yielding 0.30 g (17%). When 1.45 g (7.63 mmol) of **6a** and 2.92 g (15.4 mmol) of $(C_5H_5)_2Co$ were heated in mesitylene and worked up as described above, 0.28 g (8%) of **16a** were isolated: mp above 120 °C sublimation, above 200 °C melting; mass spectrum, *m/z* 437 (M^+, 100), 423 ($M^+ - CH_2$, 11), 189 (Cp_2Co^+, 12); high-resolution MS, *m/z* 437.1436, calcd for $^{12}C_{22}H_{33}{}^{11}B_2{}^{59}Co_2$ 437.1432 amu. Anal. Calcd for $C_{22}H_{33}B_2Co_2$: C, 60.47; H, 7.61. Found: C, 61.54; H, 7.59.

(μ-4,5-Diethyl-1,3-dimethyl-1,3-diborolenyl)bis((η^5-cyclopentadienyl)cobalt) (16b). A 0.28-g (1.03 mmol) sample of the cobalt sandwich **18b** and 0.31 g (1.72 mmol) of $(C_5H_5)Co(C_2H_4)_2$[42] in 20 mL of petroleum ether 40/60 was heated for 4 h at 40–50 °C. After the solvent was removed in vacuo, the residue was subjected to a low pressure (0.01 torr) at room temperature to remove $(C_5H_5)_2Co$, which was also formed. Then the reaction product was dissolved in petroleum ether and chromatographed on a silica gel (or Florisil) column. First small amounts of $(C_5H_5)_2Co$ appeared, followed by the olive-green **16b**, which was sublimed at 90–100 °C (0.01 torr), yielding 0.22 g (54%) of **16b**: mp 145–147 °C (recrystallized from petroleum ether, −20 °C); mass spectrum, *m/z* 395 (M^+, 100), 189 (Cp_2Co^+, 15.6), 124 ($CpCo^+$, 15). Anal. Calcd for $C_{19}H_{27}B_2Co_2$ (394.9): C, 57.79; H, 6.81. Found: C, 57.48; H, 6.91.

Preparation of (η^5-Cyclopentadienyl)cobalt(μ-4,5-diethyl-1,3-dimethyl-1,3-diborolenyl)(η^5-cyclopentadienyl)iron (17b). A slurry of 0.330 g (1.44 mmol) of $(C_5H_5)Fe(C_8H_{12})$[54] and 0.400 g (1.47 mmol) of **18b**[17] in 20 mL of benzene was stirred at room temperature for 0.5 h, then slowly heated to 90 °C, and refluxed for 1 h. After cooling to room temperature and removal of the solvent in vacuo, the residue was extracted with petroleum ether. The extract was separated into two fractions by chromatography on silica gel. From the first orange fraction 0.160 g (40%) of **18b** was recovered. From the second green fraction the solvent was removed and the residue sublimed. At 50 °C (0.01 torr) some ferrocene sublimed off, followed by a small amount of orange oil. **17b** starts to sublime at 70 °C (0.01 torr). Yield 0.160 g (28%) of green **17b**: mp sublimes above 110 °C; mass spectrum, *m/z* 392 (M^+, 100), 189 (Cp_2Co^+, 5), 186 (Cp_2Fe^+, 3), 121 ($CpFe^+$, 4). Anal. Calcd for $C_{19}H_{27}B_2CoFe$ (391.8): C, 58.24; H, 6.95. Found: C, 58.50; H, 7.14. From the residue 15 mg of the quadruple-decker sandwich $[(C_5H_5)Co(\mu\text{-}C_2B_2C)]_2Fe$[18] ("CoFeCo", $C_2B_2C \simeq$ **6b**) were isolated by recrystallization from petroleum ether. The relative yields of **17b** and CoFeCo depend on the molar ratio of the starting materials. With an excess of $(C_5H_5)Fe(C_8H_{12})$ the yield of **17b** is somewhat lower and more CoFeCo is obtained.

17b was also obtained by heating a mixture of 0.270 g (10 mmol) of **18b** and 0.200 g (0.57 mmol) of $[(C_5H_5)Fe(CO)_2]_2$ in 5 mL of mesitylene for 1 h at 160 °C. The solvent was removed in vacuo, the residue extracted with *n*-hexane, and the extract chromatographed on silica gel. The first, green-brown fraction contained some **16b**, the second fraction was sublimed at 90–100 °C (0.01 torr), yielding 92 mg (24%) of **17b**.

Reaction of $18b^-$ with $(C_5H_5)Fe(CO)_2I$. A THF solution (30 mL) of **18b** (0.320 g, 1.18 mmol) was stirred over a potassium mirror prepared from 55 mg (1.4 mmol) of K for 5 h at room temperature. The resulting yellowish solution was filtered, and a THF solution of $(C_5H_5)Fe(CO)_2I$ (0.358 g, 1.18 mmol) was added dropwise. With a slight evolution of gas a white precipitate immediately formed. The reaction mixture was fil-

(53) Binger, P. *Angew. Chem.* **1968**, *80*, 288; *Angew. Chem., Int. Ed. Engl.* **1968**, *7*, 286.

(54) Jonas, K. *Adv. Organomet. Chem.* **1981**, *19*, 97. Jonas, K.; Schieferstein, L. *Angew. Chem., Int. Ed. Engl.* **1979**, *18*, 549. L. Schieferstein, Dissertation, Ruhr-Universität Bochum, 1978.

tered and the solvent removed in vacuo. The residue was chromatographed on silica gel with petroleum ether/toluene (80:20), which yielded an orange-green solution. With THF/toluene (80:20) a bright red fraction (0.180 g (86%) of $[(C_5H_5)Fe(CO)_2]_2$) was obtained. The orange-green solution was separated into three fractions by further chromatography on silica gel with petroleum ether. From the first, an orange fraction after the removal of solvent in vacuo was recovered (0.160 g (50%) of **18b**). From the second brownish-green fraction 30 mg (15%) of the CoCo triple-decker **16b** were sublimed off at 80 °C (0.01 torr). The sublimation residue yielded after recrystallization from petroleum ether, 40 mg of the CoFeCo quadruple-sandwich complex.[18] Likewise the third green fraction, which immediately followed the second, contained 20 mg (4%) of **17b**, identified by mass and NMR spectra.

Reaction of 18b⁻ and $C_5H_5^-$ with $FeCl_2$. An ether solution (30 mL) of 0.150 g (0.43 mmol) of **15b** was stirred over a potassium mirror (80 mg, 2.0 mmol) for 7 days at room temperature. Then 0.600 g of $FeCl_2 \cdot 2THF$ (2.2 mmol) was added and stirred for 2 h. The solvent was removed in vacuo and the residue extracted with petroleum ether, from which 0.115 g (68%) of **17b** was sublimed off at 80–90 °C (0.01 torr).

(η^5-Cyclopentadienyl)cobalt(μ-2-methyl-1,3,4,5-tetraethyl-1,3-diborolenyl)(η^5-cyclopentadienyl)iron (17a) was prepared[15] in low yields (4–10%) by heating a mixture of $[(C_5H_5)Fe(CO)_2]_2$, $(C_5H_5)Co(CO)_2$, and **6a** in 5 mL of mesitylene for 5 h at 170 °C.

Reduction of the NiCo Triple-Decker 15b. An ether solution (30 mL) of 1.80 g (4.6 mmol) of **15b** was stirred over a potassium mirror (0.20 g, 5.0 mmol) for 16 h at room temperature. The solvent was removed in vacuo and the residue several times extracted with petroleum ether, which resulted in 1.1 g (80%) of dark green **20b**: mp 200 °C (petroleum ether, −20 °C); mass spectrum, m/z 600 (M^+, 100). Anal. Calcd for $C_{28}H_{44}B_4Co_2Ni$ (600.5): C, 55.96; H, 7.39. Found: C, 55.98; H, 7.48.

Oxidation of the Triple-Deckers with $Ag^+BF_4^-$. To a solution of 0.66 g (1.51 mmol) of **14a** in 10 mL of ether was slowly added a solution of 0.64 g (3.39 mmol) of $AgBF_4$ in 10 mL of ether, which immediately caused the formation of a dark solid. The addition of $AgBF_4$ was stopped when the green solution turned colorless. The reaction mixture was filtered, and the solid was washed several times with ether. The formed salt **14a**$^+BF_4^-$ was dissolved in CH_2Cl_2 in order to separate it from silver. Adding n-pentane to the green solution yielded 0.68 g (85%) of dark green powder: mass spectrum (FD), m/z 435 (**14a**$^+$, 100). Anal. Calcd for $C_{22}H_{33}B_3F_4Ni_2$ (523.4): C, 50.49; H, 6.36; Ni, 22.44. Found: C, 50.18; H, 6.19; Ni, 22.48. **14a**$^+BF_4^-$ was also obtained when 0.54 g (1.73 mmol) of **13a** was oxidized with $AgBF_4$ (0.43 g, 2.2 mmol) in ether, yielding 0.18 g (40%).

Analogous to **14a**$^+BF_4^-$ the following triple-decker salts were obtained: **15a**$^+BF_4^-$ from 0.95 g (2.18 mmol) of **15a** and 100 g (5.13 mmol) of $AgBF_4$; yield 1.05 g (92%); mass spectrum (FD), m/z 436 (**15a**$^+$, 100). Anal. Calcd for $C_{22}H_{33}B_3CoF_4Ni$ (523.6): C, 50.47; H, 6.35; Co, 11.26; Ni, 11.21. Found: C, 50.38; H, 6.29; Co, 11.24; Ni, 11.18.

16a$^+BF_4^-$ from 0.30 g (0.69 mmol) of **16a** and 0.2 g (1.03 mmol) of $AgBF_4$; yield 0.30 g (83%); mass spectrum (FD), m/z 437 (**16a**$^+$, 100). Anal. Calcd for $C_{22}H_{33}B_3Co_2F_4$ (523.8): C, 50.45; H, 6.35. Found: C, 50.13; H, 6.22.

17b$^+BF_4^-$ from 0.155 g (0.40 mmol) of **17b** and 0.114 g (0.40 mmol) of $AgBF_4$; yield 0.180 g (95%). Anal. Calcd for $C_{19}H_{27}B_3CoF_4Fe$ (478.6): C, 47.68; H, 5.69. Found: C, 46.43; H, 5.78.

Reaction between the NiCo Triple-Decker 15a and $Fe_2(CO)_9$. A 0.270-g (0.62 mmol) sample of **15a** and 0.75 g (2.06 mmol) of $Fe_2(CO)_9$ were heated in 10 mL of mesitylene at 150 °C for 6 h. The solvent was removed in vacuo and the residue dissolved in n-hexane and filtered. After removal of solvent the brownish-green reaction mixture was subjected to sublimation, which yielded green **17a** (~10%). The red residue contained the tetranuclear complex **23a**: mass spectrum (FD), m/Z 798 (M^+); IR ν_{CO} 1852 cm^{-1}. **23a** is identical with the reaction product obtained from **18a** and $Ni(CO)_4$.[21b] In refluxing toluene (4.5 h) **15a** and $Fe_2(CO)_9$ (excess) yielded several products,[21a] separated on silica: **17a**, $(C_5H_5)Co(C_2B_2C)Fe(CO)_3$ (13%); IR ν_{CO} 2052, 1988 cm^{-1} (petroleum ether); mass spectrum, m/z 452 (M^+, 50); **22a** (20%) mp 126–128 °C; IR ν_{CO} 2011, 1828 cm^{-1} (petroleum ether), mass spectrum (FD), m/z 576 (M^+, 100); **23a** (4%); $[(C_5H_5)Fe(CO)_2]_2$ (15%).

Reaction between the NiNi Triple-Decker 14b and $Fe_2(CO)_9$. A solution of 1.10 g (2.52 mmol) of **14b** and 2.0 g (5.5 mmol) of $Fe_2(CO)_9$ in 20 mL of toluene was refluxed for 2 h. The solvent was removed in vacuo and the reaction products chromatographed on silica. From the first, brown fraction in petroleum ether red-brown crystals were obtained on cooling, yielding 0.20 g (26%) of **27b**: mp 172 °C; mass spectrum (EI), m/z 632 (M^+, 9), 576 ($M^+ - 2CO$, 15), 548 ($M^3 - 3Co$, 100); IR ν_{CO} 2052, 2000, 1991 cm^{-1}. Anal. Calcd for $C_{24}H_{34}B_4Fe_2NiO_6$ (632.2): C, 45.60; H, 5.42. Found: C, 44.30; H, 5.52.

The second, red fraction contained the diamagnetic **26b** and paramagnetic **24b**, which could not be separated; both sublimed at 80–90 °C (0.01 torr), yield 0.5 g. As a third fraction (in n-hexane/benzene (10:1)) 0.15 g (11%) of **25b** was obtained: mass spectrum (EI), m/z 550 (M^+, 33), 410 ($M^+ - 5Co$, 100); IR ν_{CO} 2056, 2020, 1988, 1983, 1834 cm^{-1} (C_2Cl_4). Anal. Calcd for $C_{20}H_{22}B_2Fe_2NiO_6$ (550.4): C, 43.64; H, 4.03. Found: C, 43.81; H, 4.01. As a last fraction some $[(C_5H_5)Fe(CO)_2]_2$ was obtained by using benzene as solvent.

Reaction between the CoCo Triple-Decker 16a and $Mn_2(CO)_{10}$. A solution of 0.540 g (1.24 mmol) of **16a** and 0.60 g (1.54 mmol) of $Mn_2(CO)_{10}$ in 10 mL of mesitylene was heated at 170–180 °C for 3 h. The solvent was removed in vacuo from the red-brown reaction mixture, and the residue was dissolved in 20 mL of petroleum ether and filtered. Dark violet crystals were isolated by sublimation at 120–130 °C (0.01 torr) from the petroleum ether fraction, yielding 0.35 g (66%) of **28a**: mass spectrum (EI), m/z 428 (M^+, 11), 400 ($M^+ - CO$, 13), 372 ($M^+ - 2Co$, 100); IR ν_{CO} 2010, 1950 cm^{-1} (C_2Cl_4).

Acknowledgment. This research was supported by generous grants from the Deutsch Forschungsgemeinschaft, the Fonds der Chemischen Ind., the BASF Aktiengesellschaft, the National Science Foundation (CHE 80-04242), and the donors of the Petroleum Research Fund, administered by the American Chemical Society. We are grateful to Dr. K. Steinbach (Marburg) and Dr. R. Geist (Heidelberg) for recording the mass spectra, to Dr. S. Berger (Marburg), Dr. P. Kunzelmann, Dr. G. Schilling, and G. Rissmann (Heidelberg) for the NMR spectra, and to R. Pfeiffer (Marburg) and R. Gänzler (Heidelberg) for performing elemental analyses.

Registry No. 6a, 18067-54-4; **6b**, 81620-71-5; **13a**, 62708-15-0; **13b**, 84959-66-0; **14a**, 84959-67-1; **14a**$^+$, 84959-68-2; **14a**$^-$, 84959-69-3; **14a**$^+BF_4^-$, 84959-70-6; **14b**, 84959-71-7; **15a**, 84959-73-9; **15a**$^+$, 84959-75-1; **15a**$^-$, 84959-74-0; **15a**$^+BF_4^-$, 84959-76-2; **15b**, 84959-77-3; **16a**, 84959-78-4; **16a**$^+$, 84986-87-8; **16a**$^+BF_4^-$, 84959-80-8; **16b**, 84959-81-9; **17a**, 84959-82-0; **17a**$^+$, 84959-83-1; **14b**$^-$, 84959-72-8; **17a**$^-$, 84959-84-2; **17b**, 84959-85-3; **17b**$^+$, 84959-86-4; **17b**$^+BF_4^-$, 84986-88-9; **18b**, 81628-83-3; **20b**, 84959-87-5; **23a**, 81987-35-1; **24b**, 84959-88-6; **25b**, 84986-89-0; **26b**, 84959-89-7; **27b**, 84959-90-0; **28a**, 84959-91-1; $(C_5H_5)_2Ti(CH_2)ClAl(CH_3)_2$, 71929-87-8; $[(C_5H_5)Ni(CO)]_2$, 12170-92-2; $(C_5H_5)Co(CO)_2$, 12078-25-0; $(C_5H_5)Co(C_2H_4)_2$, 69393-67-5; $(C_5H_5)Fe(C_8H_{12})$, 70713-60-9; $(C_5H_5)Fe(CO)_2I$, 12078-28-3; $[(C_5H_5)Fe(CO)_2]_2$, 12154-95-9; $FeCl_2$, 7758-94-3; $Fe_2(CO)_9$, 15321-51-4; $(C_5H_5)Co(C_2B_2C)Fe(CO)_3$, 84986-90-3; $Mn_2(CO)_{10}$, 10170-69-1; $Cp_2Fe^+BF_4^-$, 1282-37-7; 4,5-diethyl-1,3-diiodo-Δ^4-1,2,5-thiadiborolene, 58347-18-5.

Supplementary Material Available: Listing of anisotropic thermal parameters of **14b**, **16b**, and **17b** (3 pages). Ordering information is given on any current masthead page.